Gondwana Research xxx (xxxx) 1–25

Contents lists available at ScienceDirect

Gondwana Research

journal homepage: www.elsevier.com/locate/gr

Alpha-Mendeleev Rise, Arctic Ocean: A double volcanic passive margin

Anatoly M. Nikishin[a,*], Elizaveta A. Rodina[a], Ksenia F. Startseva[a], Gillian R. Foulger[b], Henry W. Posamentier[c], Alexander P. Afanasenkov[d], Alexey V. Beziazykov[e], Andrey A. Chernykh[e], Nikolay A. Malyshev[f], Eugene I. Petrov[g], Sergey G. Skolotnev[h], Vladimir E. Verzhbitsky[f], Ilya.V. Yakovenko[e]

[a] *Geological Faculty, Moscow State University, Moscow, Russia*
[b] *Department of Earth Sciences, Durham University, Science Laboratories, South Rd. DH1 3LE, UK*
[c] *2134 Sea Way, Bodega Bay, CA, USA*
[d] *Rosgeo, Moscow, Russia*
[e] *Gramberg All-Russia Scientific Research Institute for Geology and Mineral Resources of the Ocean (VNIIOkeangeologia), Saint Petersburg, Russia*
[f] *Rosneft Oil Company, Moscow, Russia*
[g] *The Federal Subsoil Resources Management Agency, Moscow, Russia*
[h] *Geological Institute, Russian Academy of Sciences, Moscow, Russia*

A R T I C L E I N F O

Article history:
Received 25 November 2021
Received in revised form 2 September 2022
Accepted 21 October 2022

Keywords:
Arctic
Mendeleev Rise
Alpha Ridge
Podvodnikov Basin
Stefansson Basin
North Chukchi Basin
SDR
Failed micro-oceanic basins
Crustal model
Half-graben
Volcanic passive continental margin

A B S T R A C T

Data collected by several expeditions to the Arctic Ocean have yielded a seismic stratigraphic framework and basin fill history for the Alpha-Mendeleev Rise (AMR) and adjacent Podvodnikov, Makarov, North Chukchi, Toll, Mendeleev, Nautilus and Stefansson basins. The AMR comprises a double-sided volcanic passive margin formed in Aptian-Albian time. The North Chukchi, Podvodnikov, Toll, Mendeleev, Nautilus, and Stefansson basins formed synchronously with the Alpha-Mendeleev Rise as failed micro-oceanic basins. Their formation started with rifting and volcanism at ~ 125 Ma and ended at 100–90 Ma. Ages are constrained by new isotope magmatic rock ages. The region now comprising the Amerasia Basin was in an intraplate tectonic setting during Aptian-Albian times. On the Mendeleev Rise seismic units interpreted as seaward-dipping reflectors (SDRs) form wedges separated by highs. We propose an axial line along the Mendeleev Rise that separates probable half-grabens of different polarity. On the western slope of the Rise, all bright reflections have westward dips, while on the eastern slope they have eastward dips. SDR-like seismic units are common within the adjacent basins as well. Gravity/magnetic crustal modelling for two regional seismic lines demonstrate that the Mendeleev Rise and adjacent basins are associated with stretched continental crust.

1. Introduction

The Arctic Ocean comprises the Eurasia and Amerasia deep-water basins (Fig. 1), which are separated by the Lomonosov Ridge. In the Amerasia Basin, there are two major domains (Nikishin et al., 2014, 2021a) – the North Amerasia and South Amerasia domains. The South Amerasia domain is represented by the Canada Basin. The North Amerasia domain has a complex geological structure and the Alpha-Mendeleev belt of uplifts lies approximately along its axis. The Alpha Ridge was discovered 1957–1958 by the US ice station Alpha (Hunkins, 1961) and the southern part of the Mendeleev Rise was discovered in 1948 (Gakkel and Ya, 1962). By the early 1970′s, it had been shown that the Alpha Ridge and Mendeleev Rise form a single system of uplifts. Heezen and Tharp (1975) were among the first to illustrate this on an Arctic Basin seafloor terrain map. Present-day knowledge of Arctic Ocean bathymetry is presented by Jakobsson et al. (2020).

Up until the present, the Amerasia Basin has remained the least studied part of the Arctic Ocean. There are a variety of models for its geological structure and evolution to account for distribution of crustal types and chronology of geological events (*e.g.*, Bruvoll et al., 2012; Dove et al., 2010; Funck et al., 2011; Grantz et al., 2011a,b; Jokat, 2003; Dobretsov et al., 2013; Jokat and Ickrath, 2015; Døssing et al., 2013, 2017; Miller and Verzhbitsky, 2009; Laverov et al., 2013;

* Corresponding author.
E-mail address: nikishin@geol.msu.ru (A.M. Nikishin).

https://doi.org/10.1016/j.gr.2022.10.010
1342-937/© 20XX

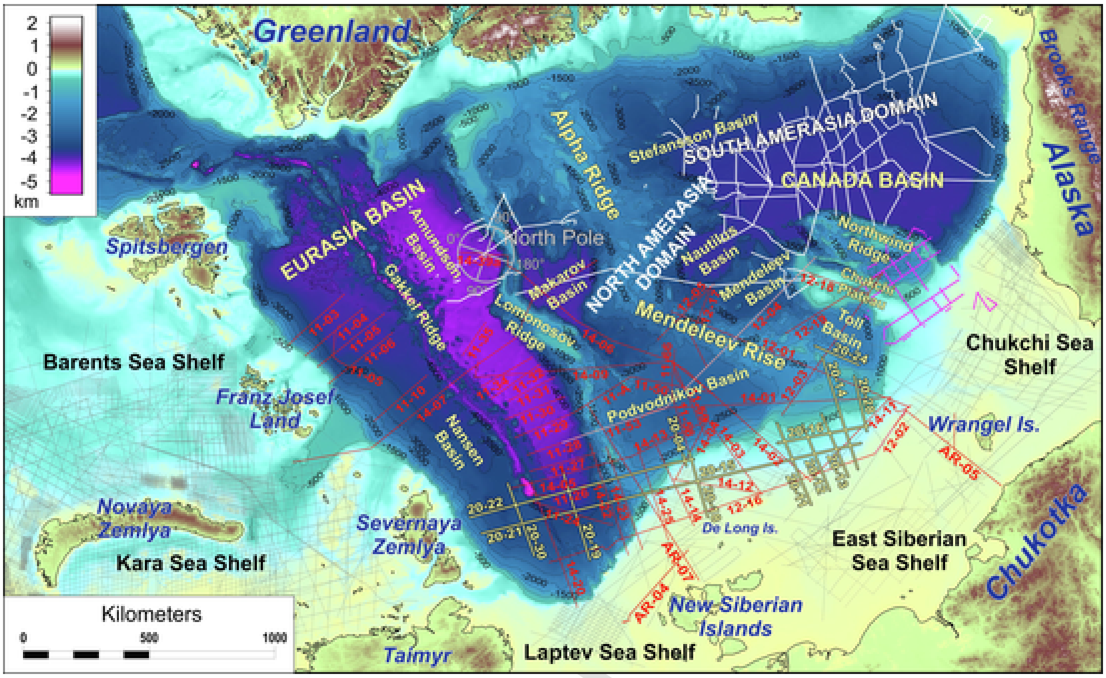

Fig. 1. Topography and bathymetry of the Arctic region (Jakobsson et al., 2020). Red lines indicate seismic data acquired during the Russian expeditions *Arktika-2011, Arktika-2012*, and *Arktika-2014*. Yellow lines indicate seismic data acquired during Russian expedition *Arktika-2020.* White lines indicate seismic data presented by the Geological Survey of Canada (Shimeld et al., 2021). Dashed white line – location of profile of Supplementary Fig. S14. (For interpretation of the references to colour in this figure legend, the reader is referred to the web version of this article.)

Nikishin et al., 2014, 2021 a,b,c; Oakey and Saltus, 2016; Petrov et al., 2016; Petrov and Smelror, 2019, 2021; Vernikovsky et al., 2014; Chian et al., 2016; Hutchinson et al., 2017; Chernykh et al., 2018, Mosher et al., 2012; Jackson and Chian, 2019; Lobkovsky et al., 2021). The Canada Basin is characterized by normal oceanic crust along its axis and widespread hyper-extended continental crust beneath its marginal parts (Mosher et al., 2012; Chian et al., 2016; Li et al., 2016; Hutchinson et al., 2017; Døssing et al., 2020). The age of the crust is disputed and different hypotheses suggest dates from Jurassic to Late Cretaceous and Paleocene (*e.g.*, Alvey et al., 2008; Grantz et al., 2011a, b; Hutchinson et al., 2017; Miller et al., 2018a, 2018b; Døssing et al., 2020).

The North Amerasia domain comprises the Alpha-Mendeleev Rise (AMR) and the Podvodnikov, Makarov, Toll, Mendeleev, Nautilus, Stefansson, and other adjacent deep-sea basins. This domain exhibits high amplitude "chaotic" magnetic anomalies (the High Arctic Magnetic High Domain or HAMH; Oakey and Saltus, 2016) believed to be associated with the High Arctic Large Igneous Province (HALIP), aged 130–80 Ma (*e.g.*, Døssing et al., 2013; Coakley et al., 2016; Oakey and Saltus, 2016; Dockman et al., 2018; Buchan and Ernst, 2018; Mukasa et al., 2020; Nikishin et al., 2021a,b,c). A fundamental question is the relationship between HALIP magmatism and the formation and geodynamics of the AMR and associated basins. Very different ideas have been suggested concerning both geological structure and chronology of events for this region as summarized by Alvey et al. (2008).

Several stratigraphic schemes exist for the Amerasia Basin (*e.g.*, Grantz et al., 2011a,b; Mosher et al., 2012; Døssing et al., 2013; Brumley, 2014; Weigelt et al., 2014; Evangelatos and Mosher, 2016; Hutchinson et al., 2017; Nikishin et al., 2014, 2021b; Poselov et al., 2017; Ilhan and Coakley, 2018; Petrov and Smelror, 2019, 2021). All differ significantly from each other and need additional testing. In this paper we use extensive seismic reflection data, supported by sample control and gravity modelling, to develop a new model for the structure and genesis of the Mendeleev Rise, Alpha Ridge and adjoining deep-sea basins.

2. Geological setting of the study area

The tectonic framework of the study area is presented in Fig. 2. The Lomonosov Ridge is a terrane characterized by continental crust which, according to reconstructions, formed from Paleozoic orogens (a continuation of the Caledonian, Timanian, and Taimyr orogens) (Jokat et al., 1992; Poselov et al., 2012; Knudsen et al., 2018; Miller et al., 2018b, 2018a; Nikishin et al., 2014; Rekant et al., 2019). The AMR crosses the Amerasia Basin between the Russian East Siberian – Chukchi Sea shelves and the shelf of islands of the Canadian Archipelago. The AMR is uplifted and has a relatively thick crust of up to 20–30 km (Funck et al., 2011; Alvey et al., 2008; Glebovsky et al., 2013; Gaina et al., 2014; Jokat and Ickrath, 2015; Lebedeva-Ivanova et al., 2019; Petrov et al., 2016; Evangelatos et al., 2017; Kashubin et al., 2018; Struijk et al., 2018; Piskarev et al., 2019). There are two main viewpoints concerning the crustal structure of this uplift (*e.g.*, Gaina et al., 2014; Pease et al., 2014). Some authors assume the zone of uplift is a Cretaceous oceanic plateau with a basaltic crust formed above a mantle plume (*e.g.*, Bruvoll et al., 2012; Dove et al., 2010; Funck et al., 2011; Grantz et al., 2011a,b; Jokat, 2003; Jokat and Ickrath, 2015). Others hold the view that this uplifted domain has a continental crust strongly thinned by rifting in which a Cretaceous plume- or mantle flow-volcanism manifested itself (*e.g.*, Døssing et al., 2013; Miller and Verzhbitsky, 2009; Laverov et al., 2013; Nikishin et al., 2014, 2021a,b,c; Oakey and Saltus, 2016; Petrov et al., 2016; Kashubin et al., 2018; Vernikovsky et al., 2014; Jackson and Chian, 2019; Lobkovsky et al., 2021). The uplifted area has complex seabed relief and in general comprises alternating basins and submarine ranges.

The crustal structure of the Makarov-Podvodnikov Basin is also disputed (*e.g.*, Evangelatos et al., 2017; Lebedeva-Ivanova et al., 2019). Some authors assume that this basin is floored by oceanic crust of unknown age (Alvey et al., 2008; Grantz et al., 2011a,b; Evangelatos et al., 2017). Others consider it to be continental crust thinned by rifting (Glebovsky et al., 2013; Jokat and Ickrath, 2015; Kashubin et al., 2018; Langinen et al., 2009; Laverov et al., 2013; Nikishin et al., 2021b,c; 2014; Petrov et al., 2016; Piskarev et al., 2019). The Nautilus-

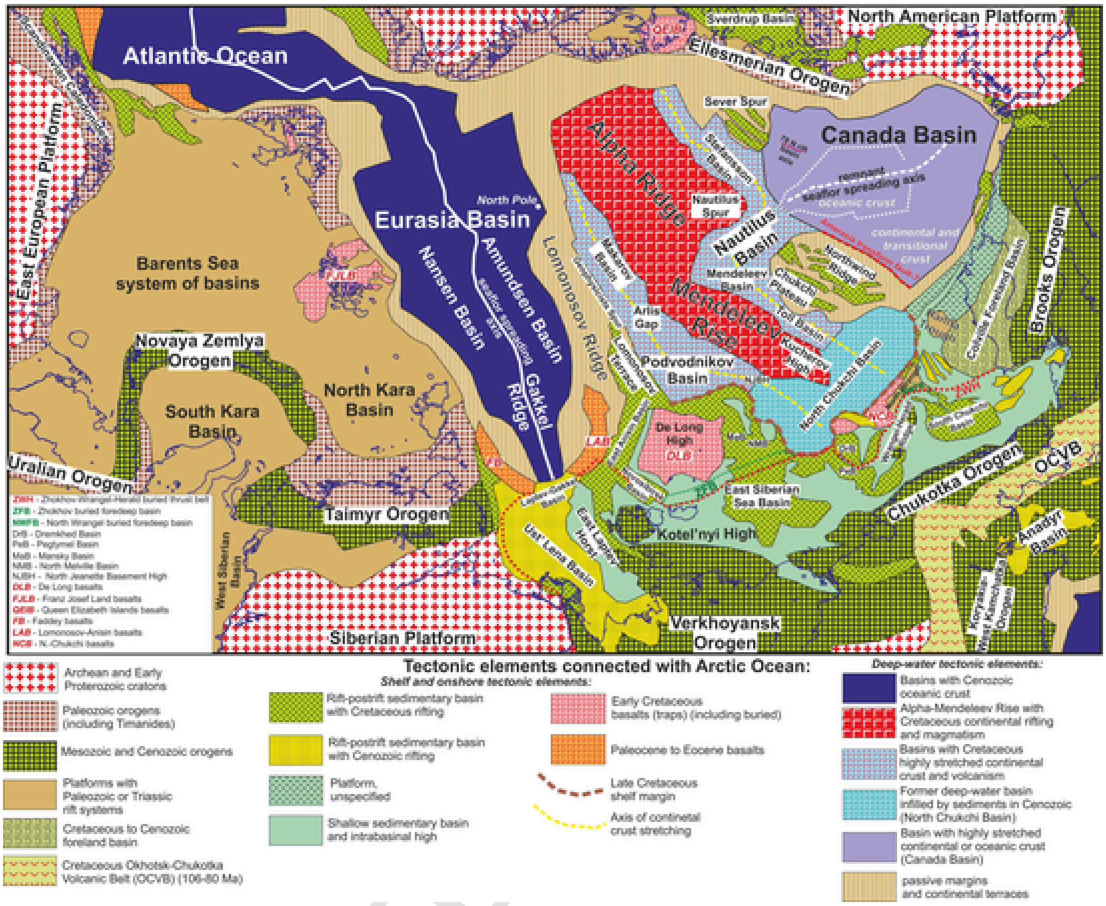

Fig. 2. Tectonic scheme of the Arctic Ocean region, based on Nikishin et al. (2014, 2021b) integrated with newly-acquired data. The Canada Basin structure has been mapped using data from Mosher et al. (2012) and Chian et al. (2016). The geographic base map is the Geological map of the Arctic (Harrison et al., 2011).

Mendeleev-Toll Basin lies between the Chukchi Plateau and the Mendeleev Rise. The structure of its crust is also debated. Some authors assume its crust is oceanic (Grantz et al., 2011a,b; Hegewald and Jokat, 2013). However, seismic data on basement topography and gravity modeling suggest it is continental and strongly extended by rifting (Brumley, 2014; Nikishin et al., 2021b,c; 2014; Chernykh et al., 2016).

The Stefansson Basin lies between the Alpha Ridge and the continental slope of the Canadian Arctic Archipelago and its Sever Spur terrace. There are few publications about this basin. It is seen as part of the HALIP unit (*e.g.*, Coakley et al., 2016). Recently published new seismic data show, however, that its structure is complicated (Shimeld et al., 2021). The Chukchi Plateau (or Chukchi Borderland) comprises a zone of uplift underlain by continental crust (Grantz et al., 1998; Alvey et al., 2008; Coakley et al., 2016; Gaina et al., 2014; Ilhan and Coakley, 2018; Kashubin et al., 2018). On the slope of the central part of the Chukchi Borderland, dredging produced igneous rocks aged ~ 428 Ma, providing evidence for early Paleozoic orogenesis in the area (Brumley et al., 2015), coeval with the Caledonian Orogeny in Europe. It appears that crust of Early Paleozoic and older age exists within this plateau (Brumley et al., 2015).

On the Laptev, East Siberian and Chukchi shelves, many Cretaceous and Cenozoic rifts have been identified (*e.g.*, Drachev et al., 2018, 2010; Franke and Hinz, 2005; Franke, 2013; Ilhan and Coakley, 2018; Nikishin et al., 2014, 2021b,c; Savin, 2020; Petrov and Smelror, 2019). These rifts extend to the continental margin of the deep-water Arctic Basin, suggesting that they and their basins formed in a single geodynamic environment.

The North Chukchi Basin lies on the north of the Chukchi Sea Shelf. This basin is particularly significant since it borders both the Mendeleev Rise and the deep-water Podvodnikov and Toll basins. The North Chukchi Basin has sedimentary cover thickness of 20–22 km and is underlain by hyper-extended continental crust (Nikishin et al., 2014, 2021a,b,c; Skaryatin et al., 2021).

3. Data and methods

The current paper is based primarily on interpretation of 2D seismic lines and magnetic and gravity analyses using data acquired through the Russian Arktika-2011, Arktika-2012, Arktika 2014, and Arktika-2020 projects under the common title *Arctic Ocean Mega Project* (Nikishin et al., 2021a,b,c). The seismic data are described by Nikishin et al. (2021a) and the lines are shown in Fig. 1. We incorporate results of seismic sonobuoy data published in technical reports and papers (*e.g.*, Butsenko et al., 2019; Petrov and Smelror, 2019; 2017; Poselov et al., 2019, 2012). We make extensive use of the results of the deep-water geological expeditions of 2014 and 2016 (*Mendeleev-2014* and *Mendeleev-2016*) during which rock samples were taken from four slopes of seamounts within the Mendeleev Rise using special deep-sea vehicles. Results of these operations were partly published by Skolotnev et al. (2019, 2022) and Nikishin et al. (2021a). For the Russian and American shelves, we utilized seismic lines acquired by the companies MAGE (Murmansk, Russia), DMNG (Yuzhno-Sakhalinsk, Russia), SMNG (Murmansk, Russia), ION-GXT (USA), ROSGEO (Russia), and others. For the seismic-stratigraphic model of the Russian part of the shelf, we used all seismic lines available from the Ministry of Natural Resources and Environment of the Russian Federation.

The Geological Survey of Canada (GSC) organized several expeditions to the Amerasia Basin, mainly within the Canada Basin, 2007–2016. New seismic profiles were acquired in its deep-water part. Key data were published by Shimeld et al. (2021). Seismic data interpretations were published by Shimeld et al. (2011), Mosher et al. (2012), Brumley (2014), Chian et al. (2016), Evangelatos and Mosher (2016), Coakley et al. (2016), Hutchinson et al. (2017). The United States Geological Survey (USGS) worked in cooperation with the GSC and other organizations. The USA National ScienceFoundation also funded expeditions to the Arctic Ocean organized by the University of Alaska, the key seismic data interpretation results of which were published by Dove et al. (2010), Bruvoll et al. (2010, 2012) and Ilhan and Coakley (2018).

The Alfred Wegener Institute for Polar and Marine Research (Germany) also organized expeditions to the Amerasia Basin. Key seismic data interpretation results were published by Weigelt et al. (2014) and Jokat and Ickrath (2015). Gravity and magnetic data were summarized by Gaina et al. (2011), Saltus et al. (2011), Døssing et al. (2013), Oakey and Saltus (2016), and Piskarev et al. (2019).

3.1. Seismic stratigraphy

A seismic stratigraphic framework for the Amerasia Basin was established by Nikishin et al. (2021b) on the basis of data from: (1) drilling the Lomonosov Ridge acquired within the ACEX Project; (2) the ages of linear magnetic anomalies of the Eurasia Basin; (3) the age of the sedimentary cover of the Chukchi Sea Shelf tied to wells; (4) the formation history of Mesozoic orogens on islands in the East Siberian and Chukchi Seas; (5) the ages of the De Long and AMR basalts, which are a part of the Alpha-Mendeleev LIP or HALIP, and (6) climate stratigraphy. The following major seismic boundaries were identified (Nikishin et al., 2014, 2017, 2019, 2021b:

1. ±125 Ma. Start of rifting in the basins of the Chukchi and East Siberian seas. Start of HALIP magmatism on the shelves of the AMR. This boundary approximately corresponds to the Base Torok unconformity (or Brookian unconformity) on the Alaska Shelf according to Sherwood et al. (2002), Craddock and Houseknecht (2016), and Homza and Bergman (2019).
2. ±100 Ma. The rift-postrift boundary in the North Chukchi Basin and in the basins of the East Siberian and Laptev seas. This boundary approximately corresponds to the top of SDR complexes in the region of the Mendeleev Rise and the Podvodnikov and Toll basins. The boundary, which may be diachronous, approximately corresponds to the Intra-Early Cenomanian unconformity on the Alaska Shelf according to Craddock and Houseknecht (2016) and Homza and Bergman (2019).
3. ±80 Ma. This horizon is drawn at the top of the high-amplitude reflection sequence-2 (HARS-2). This boundary corresponds to the start of regional uniform subsidence of the Podvodnikov Basin and, possibly, to the cooling of the Arctic (Schröder-Adams, 2014) and termination of volcanism in the AMR region (Coakley et al., 2016; Mukasa et al., 2020).
4. ±66 Ma. This horizon is interpreted along the base of the lower clinoform complex of the North Chukchi Basin and corresponds to the mid-Brookian (MBU) or Cretaceous-Paleocene (KPu) unconformity on the Alaskan Shelf (*e.g.*, Sherwood et al., 2002; Craddock and Houseknecht, 2016; Ilhan and Coakley, 2018; Homza and Bergman, 2019). This boundary may be diachronous.
5. ±56 Ma. This horizon is drawn as the rift-postrift boundary in the area of the Lomonosov Ridge and corresponds to the breakup unconformity of the Eurasia Basin. It is traced in most parts of the Arctic Ocean along the bottom of the high-amplitude reflection sequence-1 (HARS-1). It approximately corresponds to the Paleocene-Eocene Thermal Maximum (PETM) and is identified on the Alaska Shelf by Homza and Bergman (2019). Posamentier et al. (in preparation) has described possible carbonate buildups on the Mendeleev Rise lying directly on this boundary at 56 Ma and the PETM.
6. ±45 Ma. This boundary corresponds to the top of the high-amplitude reflection sequence-1 (HARS-1). It clearly corresponds to the bottom of the upper clinoform complex of the North Chukchi Basin. Posamentier et al. (in preparation) has described possible carbonate buildups on the Mendeleev Rise whose tops coincide with the proposed 45 Ma boundary.
7. ±34 Ma. This boundary is traced along the top of the chaotic horizon on the East Siberian and Chukchi Sea shelves that corresponds to paleogeographic restructuring in the region of the Amerasia Basin. The boundary corresponds to the Terminal Eocene unconformity on the Alaska Shelf according to Homza and Bergman (2019).
8. ±20 Ma. This boundary is interpreted as an erosional event characterized by subaqueous mass failures on slopes. It corresponds to an early Miocene onset of a ventilated circulation regime in the Arctic Ocean attributed to the opening of the Fram Strait as proposed by Jakobsson et al. (2007). This boundary approximately corresponds to the base of Miocene deposits and an erosional surface in the ACEX holes on the Lomonosov Ridge (18.2 Ma), according to Jakobsson et al. (2007) and Backman et al. (2008).

This seismic stratigraphic framework is similar to that of Weigelt et al. (2020) for deposits younger than 56 Ma in the region of the Lomonosov Ridge. There are significant uncertainties in correlation with the Canada Basin seismic stratigraphy presented by Mosher et al. (2012). The main regional horizons correlated by Mosher et al. (2012) are R40 (nearly Paleocene-Eocene, 56 Ma), R30 (nearly Eocene-Oligocene boundary, 34 Ma), and R10 (nearly base Miocene).

3.2. Interpretation of the 2D seismic data

3.2.1. Acoustic basement relief and sedimentary cover thicknesses

We constructed a map of acoustic basement relief for the region using all the Russian and Canadian seismic lines for most of the Amerasia Basin as well as for the East Siberian and Chukchi Sea shelves (Fig. 3). Our map improves understanding for the shelf area by integration of many new seismic lines that recently have become available. In contrast, in the deep-water part of the Arctic Ocean we can identify only major structures. Because of the new seismic data, our maps are more detailed for the region of the AMR than those published earlier (Petrov et al., 2016; Struijk et al., 2018; Piskarev et al., 2019; Lebedeva-Ivanova et al., 2019; Mosher and Hutchinson, 2019). The map of sedimentary cover thickness was constructed using the same newly-acquired data (Supplementary Fig. S1). Mapping was performed using Petrel software.

3.2.1.1. Seismic lines. We studied the AMR region by constructing a number of composite seismic lines, as follows:

Composite Line-1 runs from the Lomonosov Ridge and crosses the southern parts of the Podvodnikov Basin, the Mendeleev Rise, the Toll Basin and the Chukchi Plateau (Fig. 4). On this line, three major units are distinctly identifiable: (1) acoustic basement, (2) synrift deposits, and (3) postrift deposits. Synrift deposits are characterized by SDR-like seismic units with a wedge-shaped architecture that is clearest in the Toll and Podvodnikov basins (Nikishin et al., 2021a,b) and on the Mendeleev Rise. Examples are shown in Fig. 4. In general, the synrift deposits fill half-grabens. The synrift-postrift boundary is distinctly identifiable and is characterized by angular discordance. In the postrift deposits, four units can be identified with tentative ages of 100–80 Ma, 80–45 Ma, 45–20 Ma, and 20–0 Ma. The 100–80 Ma deposits show increased thickness on the Lomonosov Terrace and in the Podvodnikov and Toll basins. They are markedly thin, and in some locations absent, on the higher elevations of the Mendeleev Rise, Chukchi Plateau, and Geophysicists Spur. Deposits with ages of 80–45 Ma uniformly cover al-

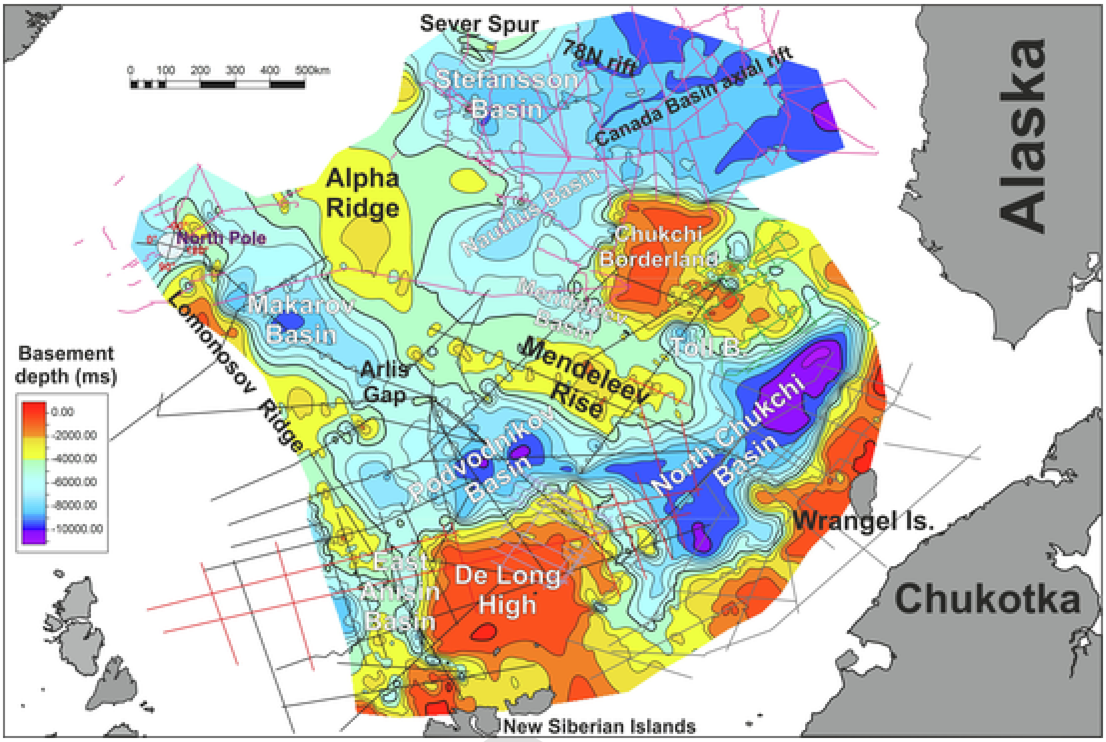

Fig. 3. Basement time-depth map compiled using interpretation of 2D seismic lines acquired during different Arctic expeditions. For the southern margin of the North Chukchi Basin and to the south of the De Long High the map was constructed using the base Aptian sediments. Digital map is presented in supplementary data-1.

most the entire region, though they strongly thin or wedge out completely in the area of the Mendeleev Rise. Deposits of 45–20 Ma are thick in the Podvodnikov Basin and thin or absent along the Lomonosov Ridge and the Mendeleev Rise. Deposits aged 20–0 Ma cover the entire territory approximately uniformly.

Composite Line-2 extends from the Lomonosov Ridge and crosses central parts of the Podvodnikov Basin and the Mendeleev Rise and the northern part of the Toll Basin and the Chukchi Plateau (Supplementary Fig. S2). On the whole, we identify the same units as on Line-1 (Fig. 4), with the following differences: (1) in the Podvodnikov Basin, SDR-like units are not readily identifiable; (2) on the Mendeleev Rise, SDR-like seismic units are clearly observed; (3) in the Toll Basin, half-grabens with distinct SDRs are not identified, though an axial V-shaped trough is unambiguously observed.

Line-3 runs along the Mendeleev Rise orthogonal to Lines 1 and 2 (Supplementary Fig. S3). On this line, we see the same major structural units. Synrift deposits are readily identifiable in the form of half-graben fills but apparent SDR units are almost absent. On this line, probable young faults (i.e., post 45 Ma) are clear and create the present-day basin-and-range relief that characterizes the Mendeleev Rise (Nikishin et al., 2014, 2021b).

Composite Line-4 runs in a near-east–west direction along the North Chukchi Basin and across the rift system of the East Siberian Sea (the Mansky and North Melville basins). These have a near-north–south trend (Supplementary Fig. S4). Interpretation of Composite Line 4 suggests: (1) the East Siberian Sea rifts and the North Chukchi Basin together form a single extensional basin system, certainly before 80 Ma if not before 100 Ma; (2) the base of the North Chukchi basin, when flattened, is free of grabens (Supplementary Fig. S4, b and c); (3) the North Chukchi Basin is traversed by a near-north-to-south uplift of the acoustic basement, which divides the basin into the West North Chukchi and the East North Chukchi basins; (4) an acoustic basement uplift named the Kucherov High (it is overlain by the Kucherov Terrace) represents a continuation of the Mendeleev Rise structure. It is possible that the acoustic basement is directly overlain by postrift sediments and a sub-horizontal detachment or décollement may occur at the base of the postrift sediments. (5) On the slopes of the Kucherov High, onlapping sediments are observed and the Rise is covered by sediments of presumed age ~ 100–90 Ma. The implication is that the Kucherov High, a continuation of the Mendeleev Rise, ceased to develop at ~ 100–90 Ma.

Composite line-5 runs first across the Mendeleev Rise, crosses a part of the Podvodnikov Basin, and subsequently terminates in the North Chukchi Basin (Supplementary Fig. S5). Within the North Chukchi Basin, the line crosses the Kucherov High at the southern termination of the Mendeleev Rise. An interpretation of this line suggests the following: (1) the rift-postrift boundary (or top of the SDR-like seismic unit) of the Mendeleev Rise in the North Chukchi Basin constitutes the top of the acoustic basement there; (2) the Kucherov High is present on this line, and the top of the associated acoustic basement approximately corresponds to the top of the SDRs of the Mendeleev Rise; (3) on the slope of the Mendeleev Rise, the top of the SDRs (±100 Ma) merges with the 80 Ma boundary (Supplementary Fig. S5, b). In contrast, deposits of 100–80 Ma age in the North Chukchi Basin are significantly thicker.

Composite Line-6 runs from the Lomonosov Ridge, across the Makarov and Podvodnikov basins, and terminates at the Mendeleev Rise (Supplementary Fig. S6). Interpretation of this line suggests the following: (1) on the southern slope of the Makarov Basin and in the area of the Arlis Gap High, numerous buried seamounts are identified. We consider them to be edifices of probable volcanic nature (Nikishin et al., 2021b) older than 80 Ma. These edifices are up to 0.5–1 s high with no associated erosion (*e.g.*, truncated volcano tops) observed, suggesting that the volcanism was subaqueous; (2) on the slope of the Mendeleev Rise, SDR-like seismic units are observed, but no large buried volcanic edifices in the form of seamounts are identified.

Composite Line-7 crosses the western part of the North Chukchi Basin and reaches the southern part of the Mendeleev Rise (Supplementary Fig. S7). Interpretation of this line yields the follow-

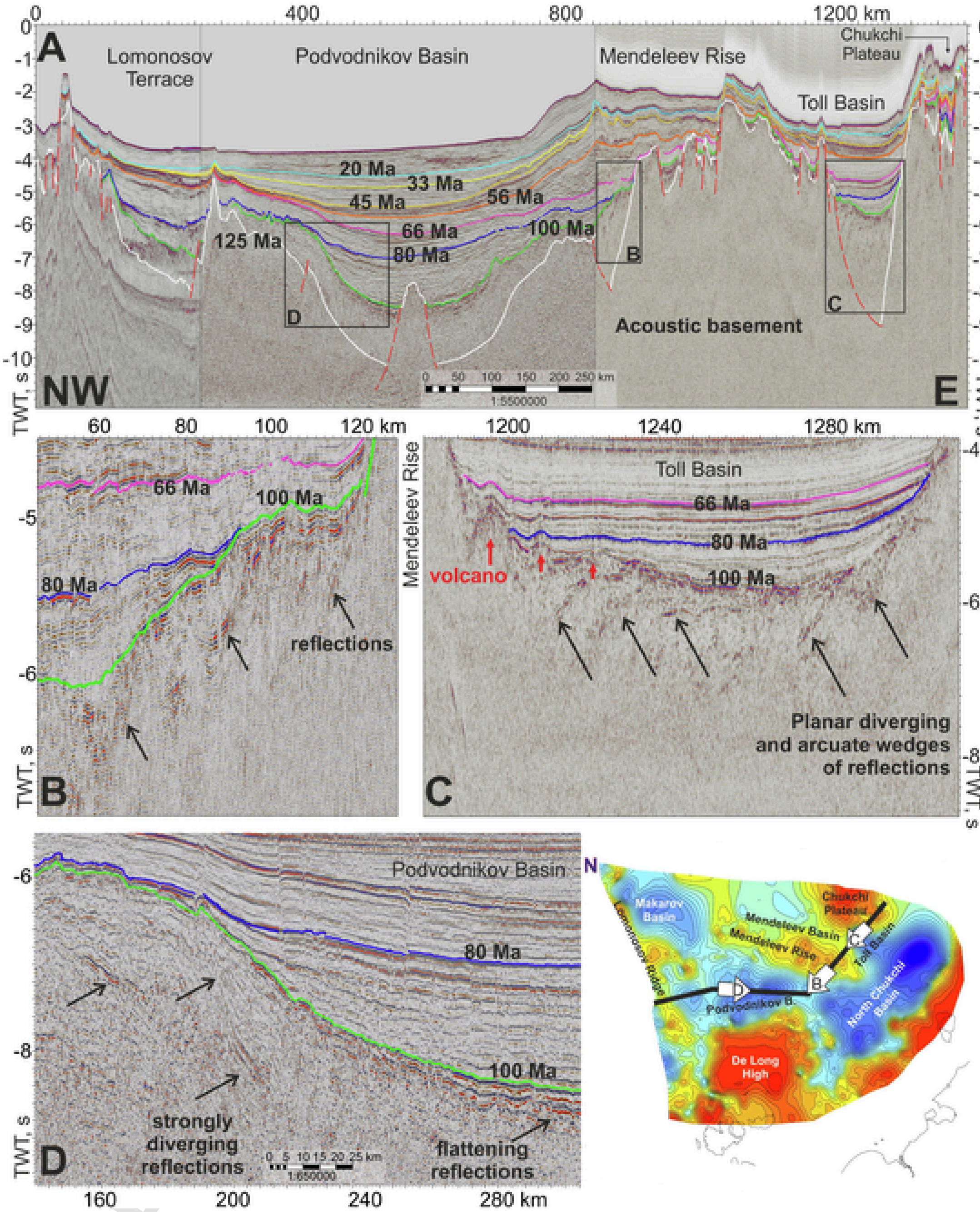

Fig. 4. A. Composite seismic line-1 and its interpretation (lines ARC 11-053, ARC 14-01, ARC 12-03). B, C and D – details of the seismic line. Seismic horizons are labeled by age. Location of the line is shown on a basement time-depth map.

ing. (1) on the northern flank of the North Chukchi Basin, several half-grabens with bright reflections are identified at the base of the section. It is possible that 125–100 Ma HALIP basalts (SDR-like seismic units) are present; (2) the rift-postrift ~ 100 Ma boundary in the half-grabens is the acoustic basement top in the deepest part of the North Chukchi Basin; (3) a thick sedimentary sequence aged ~ 100–66 Ma sharply thins out toward the Mendeleev Rise and is probably absent on the Rise itself.

Composite Line-8 crosses the North Chukchi Basin in a south-to-north direction traversing the Toll Basin and the slope of the Chukchi Plateau (Fig. 5). This line connects the Russian (the North Chukchi Basin) and American seismic data (the Toll Basin and the slope of the Chukchi Plateau) published by Ilhan and Coakley (2018). At the base of the Toll Basin, Ilhan and Coakley (2018) identified SDRs of Jurassic age. According to our correlations and age-assignments, however, these SDRs are 125–100 Ma and were formed in the HALIP epoch. For the Toll Basin, the American data show a distinct rift-postrift boundary along the top of the SDR complex (Fig. 5). In the North Chukchi Basin, the synrift complex of the Toll Basin passes into the acoustic basement. The base of the sedimentary section in the North Chukchi Basin seen on the seismic line occurs at the rift-postrift boundary of the Toll Basin (circa 100 Ma). Toward the Chukchi Plateau, the thick sedimentary unit aged 100–66 Ma wedges out completely.

Composite Line-9 crosses the western slope of the Mendeleev Rise in two places and runs along the northern flank of the North Chukchi Basin (Supplementary Fig. S8). On two slopes of the North Chukchi Basin, we observe evidence for half-graben complexes containing SDR-like seismic units. The rift-postrift boundary is distinct along the top of

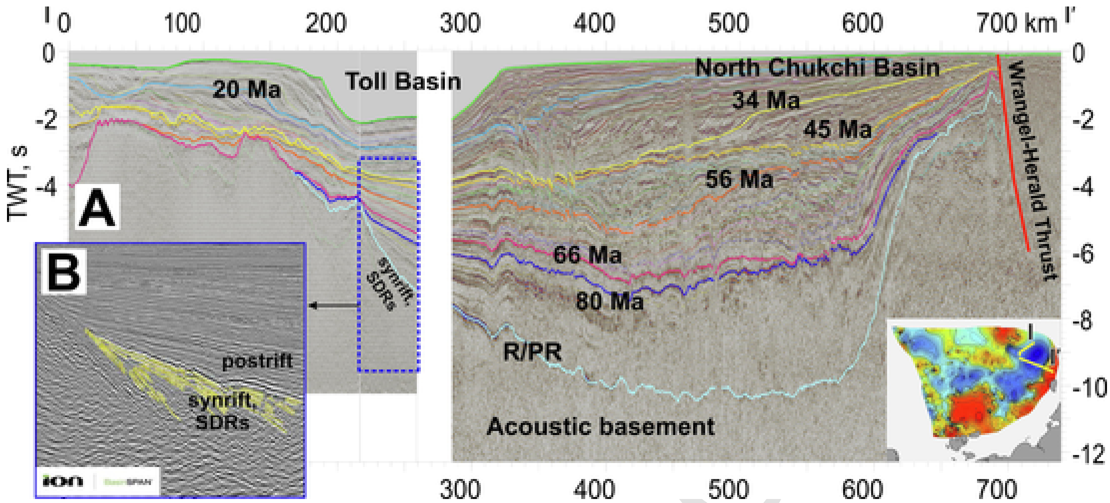

Fig. 5. A. Composite seismic line-8 and its interpretation. Right part – our seismic data (line ION 11-4200A), left part – seismic data from Ilhan and Coakley (2018). B - details of the seismic line and interpretation from Ilhan and Coakley (2018). Seismic horizons are labeled by age. R/PR – rift-postrift boundary. Location of the line is shown on a basement time-depth map.

these deposits. The interpretable section of the North Chukchi Basin begins at the rift-postrift boundary (circa 100 Ma). Below that boundary, we interpret SDR-like seismic units as half-grabens likely containing basalts of 125–100 Ma age.

Composite Line-10 crosses the western slope of the Alpha Ridge (Nautilus Spur) and runs across the Stefansson Basin toward Sever Spur continental terrace of the Canada continental margin (Fig. 6). We observe indications of half-graben complexes containing SDR-like seismic units. The rift-postrift boundary (or top of SDRs) is distinct along the top of these deposits. We interpret SDR-like seismic units as half-grabens likely containing basalts of 125–100 Ma age. A basement high is clear within the axial part of the Stefansson Basin. This high could be an axial continental high. About this possible basement high SDR-like complexes are symmetrical for both slopes of the Stefansson Basin.

Composite Line-11 is nearly coincident with Line-10 except for the Alpha Ridge slope (Supplementary Fig. S9). We observe half-graben complexes containing SDR-like seismic units on the Alpha Ridge slope. The rift-postrift boundary (or top of the SDRs) is distinct along the top of these deposits. Shimeld et al. (2011) interpreted a fragment of this profile for the Alpha Ridge slope. They marked a prominent angular unconformity (our top-SDR boundary). Above this angular unconformity they separated a regional "bisque" seismic unit. Shimeld et al. (2011) proposed that this bisque unit post-dates extrusive volcanism. They suggest that the bisque unit comprises biosiliceous oozes interbedded with clays and volcaniclastics and pyroclastics. They proposed an age of Aptian to Campanian (Cretaceous). We propose that the bisque unit comprises the first rift/postrift sedimentary unit younger than 100 Ma. It could consist of shallow-marine deposits with possible carbonates that have the same age as the HARS-2 unit within the Podvodnikov Basin (see Supplementary Fig. S2).

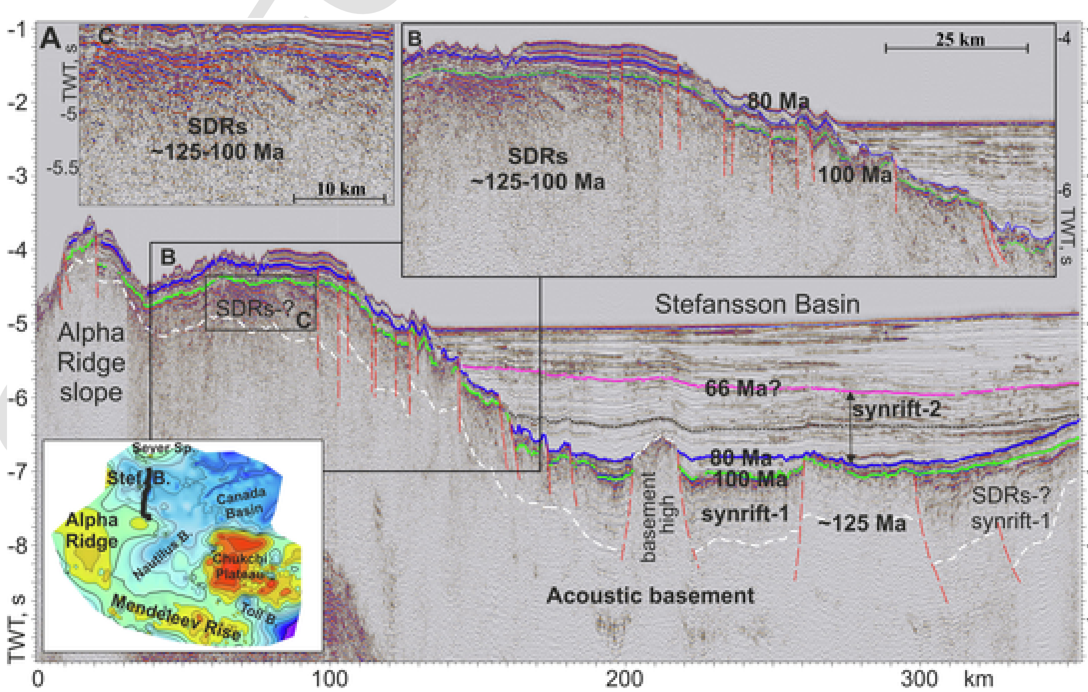

Fig. 6. A. Composite seismic line-10 and its interpretation (lines lsl-1606, lsl-0917, lsl-0918, lsl-0808a, lsl-1108). Seismic data are from Shimeld et al. (2021). B and C– details of the line and its interpretation. Seismic horizons are labeled by age. Location of the line is shown on a basement time-depth map.

We recognize a young system of normal faults, which cut the top-SDR (or rift-postrift) boundary and bisque unit and propose that rifting, with concurrent basin subsidence and rift shoulder uplift, took place after deposition of the bisque unit (~80–66 Ma). A graben system was recognized along Sever Spur (Hutchinson et al., 2017). Our seismic correlations show that the normal faults associated with these grabens cut the top-SDR (or rift-postrift) boundary within the Stefansson Basin, suggesting that the graben system of the Sever Spur is younger than HALIP tectonic and magmatic events within the Stefansson Basin and on the Alpha Ridge. It is possible that rifting on the Alpha Ridge slope and the Sever Spur took place simultaneously. Hadlari and Issler (2019) infer, on the basis of apatite fission track data from a single Cambrian sandstone sample from northern Axel Heiberg Island, rapid cooling in the Late Cretaceous with a central cooling age of 77.1 ± 5.1 Ma. It is possible that older rift structures related to opening of the Amerasia Basin were reactivated leading to rift-shoulder uplift in the Late Cretaceous. We propose that uplift of the Canadian Archipelago and a rift event or events in the region of the Stefansson Basin and the Alpha Ridge were simultaneous in the Late Cretaceous after ~ 80 Ma as predicted by Hadlari and Issler (2019).

Composite Line 12 is also lies between the Alpha Ridge and Sever Spur (Fig. 7). The Sever Spur continental slope has a possible SDR-like seismic unit. A bottom bisque or HARS-2 unit is the top of the SDRs (the rift-postrift boundary). An obvious graben system occurs in the center part of the Stefansson Basin. Normal faults cut the top of the bisque (or HARS-2) unit. Thus, rifting started nearly at 80 Ma. The rift-postrift boundary could date to near end-Cretaceous time.

Composite Line 13. Hutchinson et al. (2017) described the 78 N Basin as a graben system within the Canada Basin. We correlate the age of this graben system with events in the Stefansson Basin (Fig. 8). Our correlations demonstrate that normal faulting took place after deposition of the bisque or the HARS-2 unit. Consequently, we propose that rifting in the Stefansson Basin and on its slopes took place simultaneous with development of the 78 N graben system at ~ 80–66 Ma.

Line-14 is located between the northernmost part of Northwind Ridge (Chukchi Borderland) and the Canada Basin. This profile was interpreted by Hutchinson et al. (2017). They recognized syn- and postrift complexes above transitional crust. Our interpretation of the same seismic line (Supplementary Fig. S10) is that the so-called transitional crust displays an SDR-like seismic character and that its top is the rift-postrift boundary.

Late Paleocene-Early Eocene carbonate buildups on seismic lines and refinement of the regional seismic stratigraphic framework. On seismic line 20–24 of the *Arktika – 2020* expedition, we identified carbonate buildups (Posamentier et al., in preparation) (Fig. 9). Two types of mounds are observed – small conical-shaped features approximately 100–500 m in diameter and 50–100 m in height, and larger, massive mounds or platforms up to 3–7 km in diameter and 400 m in thickness. The smaller mounds overlie a continuous, essentially featureless (i.e. likely planar horizontal at the time of deposition) high-amplitude reflection and are widespread across the paleo-bathymetric high. Internally, the larger mounds or platforms are characterized by internal horizontal reflections indicative of aggradational accretion of shallow-water carbonate deposits. Temporally, the small mounds are overlain by much larger mounds or platforms which in some places are conical-topped and in others flat-topped. In places they are characterized by internal horizontal reflections.

These interpreted high-relief buildups lie directly above a package of planar parallel seismic reflections which, in turn, lie above basement. This suggests that these high-relief features significantly post-date basement structural stabilization, representing a temporal trend that also has been observed in other studies (Posamentier et al., 2010) and is characterized here as 1) platform dominated by small patch reefs, 2) coalescence of patch reefs into a large “mega-platform”, and 3) rapid aggradation (due to sea-level rise) and eventual submerging. The locations of these high-relief features, interpreted as carbonate buildups, is consistent with their having nucleated on these bathymetric highs. According to our seismic stratigraphic framework, these carbonates should be 56–45 Ma. The 56 Ma horizon corresponds to the PETM, whereas the Early Eocene (45 Ma) represents the Early Eocene Climate Optimum (EECO). The time interval 56–45 Ma has been characterized as subtropical and associated with the hottest period of the Cenozoic. This provided an environment favorable for carbonate formation (*e.g.*, Backman and Moran, 2009; Stein, 2019). These climate and lithologic associations lend credence to the interpretation of these boundaries as 56 and 45 Ma in age.

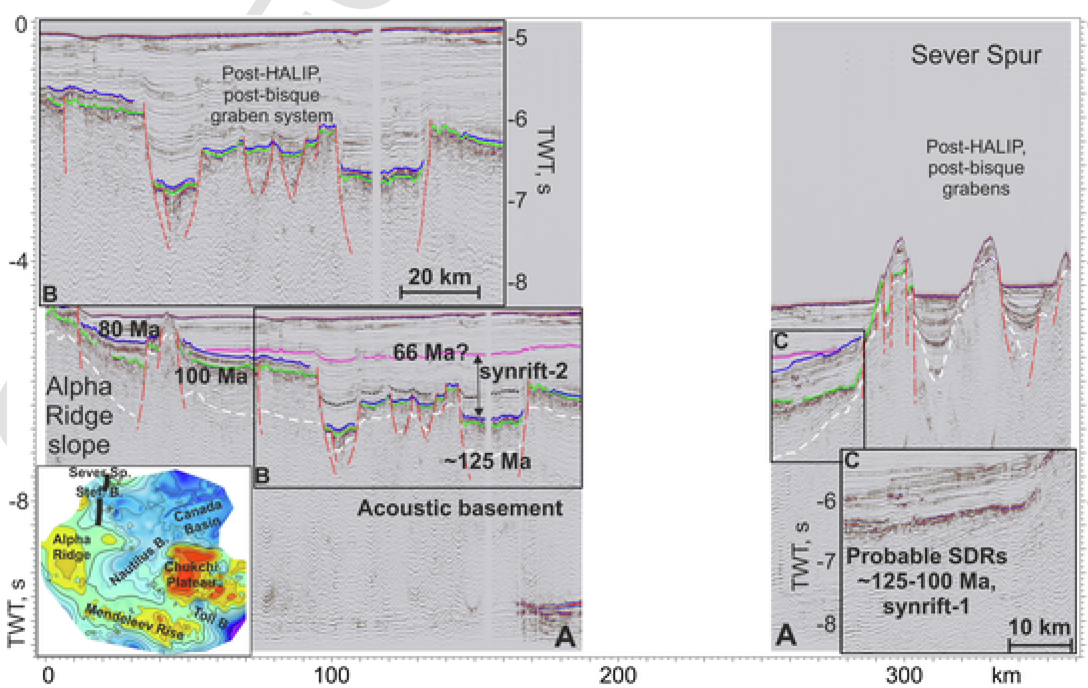

Fig. 7. A. Composite seismic line-12 and its interpretation (lines lsl-1017, lsl-1107). Seismic data are from Shimeld et al. (2021). B and C– details of the line and its interpretation. Seismic horizons are labeled by age. Location of the line is shown on a basement time-depth map.

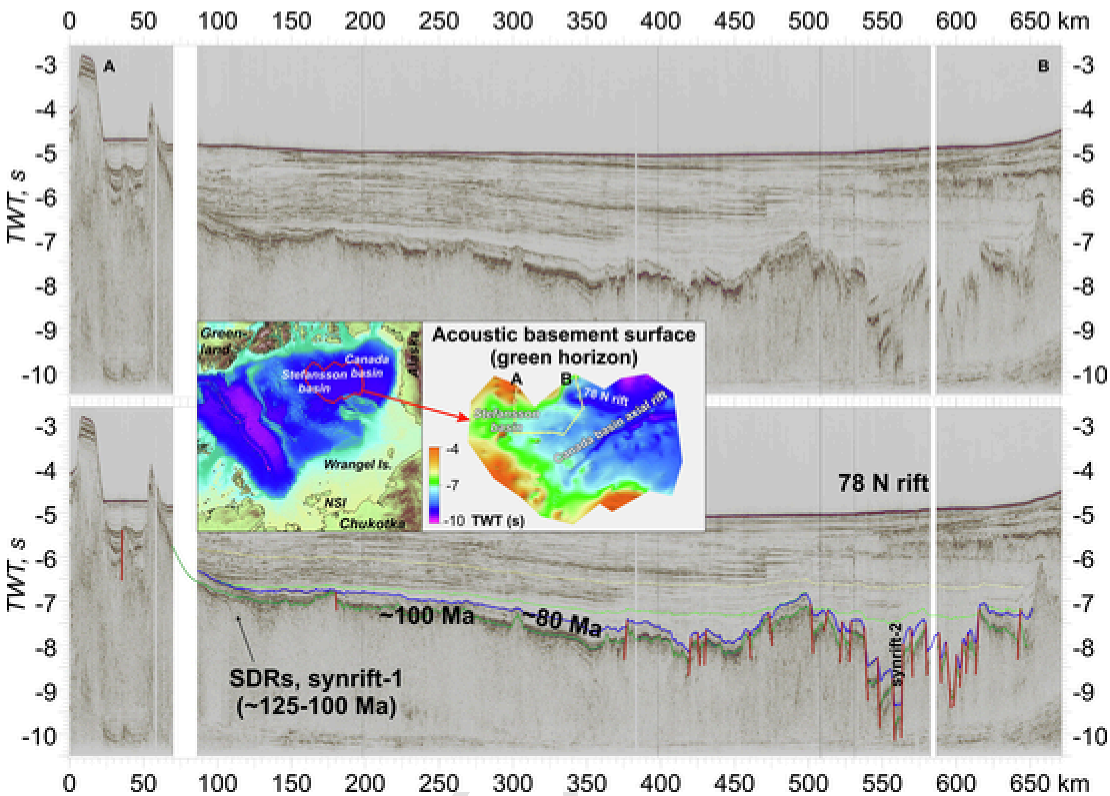

Fig. 8. Composite seismic line-13 and its interpretation (lines Isl1108, Isl0808a, Isl0925, Isl0926, Isl0927, Isl0811b, Isl0811a). Seismic data are from Shimeld et al. (2021). Seismic horizons are labeled by age. Location of the line is shown on a basement time-depth map.

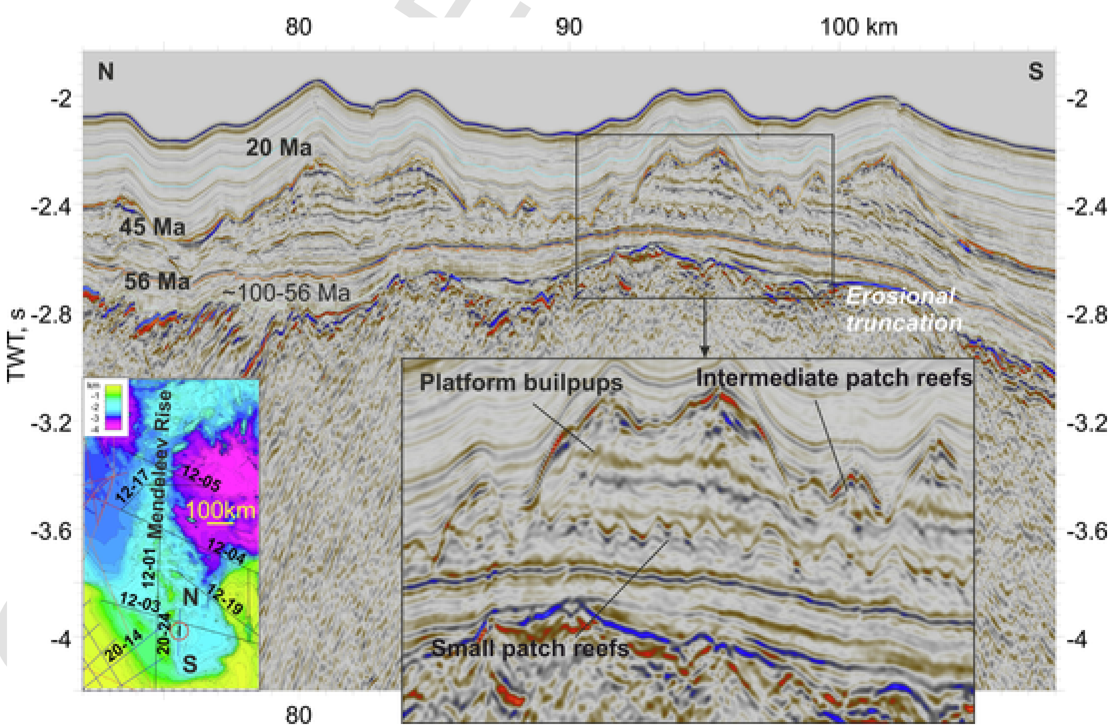

Fig. 9. Fragment of seismic line *Arktika – 2020* (line ARC 20–24) and its interpretation. A sequence of possible carbonates with two levels was proposed by Posamentier et al. (in preparation). The small buildups commonly are ~ 100–500 m in diameter and 50–100 m in height. The larger platforms are up to 3–7 km wide and up to 400 m in thickness. Some of the larger buildups are characterized by internal horizontal or aggradational architecture. Location of the profile is shown on map by circle.

We constructed a composite seismic line that ties the regions with probable carbonates on the Mendeleev Rise to the top of an extensive progradational system in the North Chukchi Basin (Supplementary Fig. S11). The apparent inundation surface that marks the culmination of progradation in the North Chukchi Basin likely represents a major flooding event, which is consistent with the presence of an apparently similar surface at the top of the interpreted carbonates. The data on the age of the carbonates helps to confirm the position of the 56 and 45 Ma boundaries in the North Chukchi Basin.

Basaltic complexes and rifts of the De Long High. On the seismic lines of the *Arktika – 2020* expedition, bright reflections are clear within the acoustic basement (Fig. 10). We interpret them as a complex of De Long basalts alternating with sedimentary rock deposits. Many half-grabens with bright reflections are readily apparent. We propose that basalts

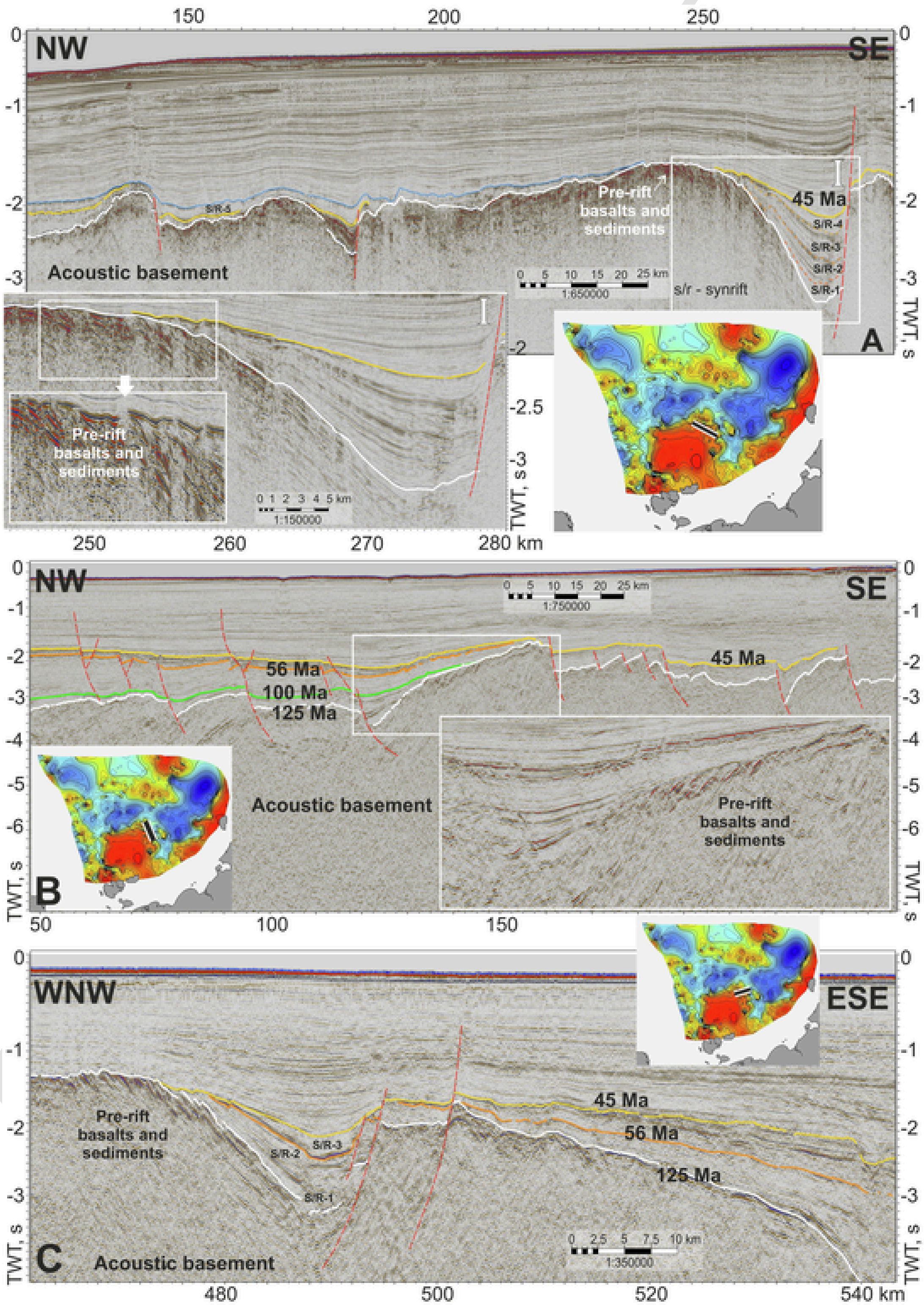

Fig. 10. Seismic lines and associated detailed views for the eastern part of the De Long High, Arktika-2020 project (A, B, C, lines ESS 16–07, ARC 20–11, ARC 20–15). Seismic horizons are labeled by age. Location of the line is shown on a basement time-depth map. S/R – synrift.

and sediments comprise the fill of these half-grabens. The formation of the half-grabens was somewhat later than the main phase of basaltic volcanism. The De Long basaltic plateau is a part of the HALIP and likely formed approximately synchronously with the volcanism of the Mendeleev Rise.

3.3. Converting 2D seismic time lines into depth lines

There are insufficient data at present for the Arctic Ocean to directly convert time to depth for the seismic lines. Accordingly, the DSS-MCS profile Arktika-2012 (Ark-1203), for which Kashubin et al. (2018) created a velocity model and presented the methodology, has been used for this. Our seismic line interpretation with time converted to depth is shown in Fig. 11. The key highlights of this line include: (1) the thickness of SDR-like units is 1–3 km, and (2) possible igneous edifices associated with SDR-like units are ~ 400–800 m high.

3.4. Distribution of SDR-like units, volcanoes and other features

We studied dips of reflections within synrift deposits using all the 2D seismic lines in the area of the AMR and adjacent basins (Figs. 12 and 13). Three principal types of reflections have been identified: (1) dipping SDR-like units; (2) dipping isolated bright reflections in presumed half-grabens; and (3) dipping half-graben bases. Although 2D data do not enable estimates of the true dip directions of reflections we nonetheless see the following patterns: (1) for the Mendeleev Rise, we

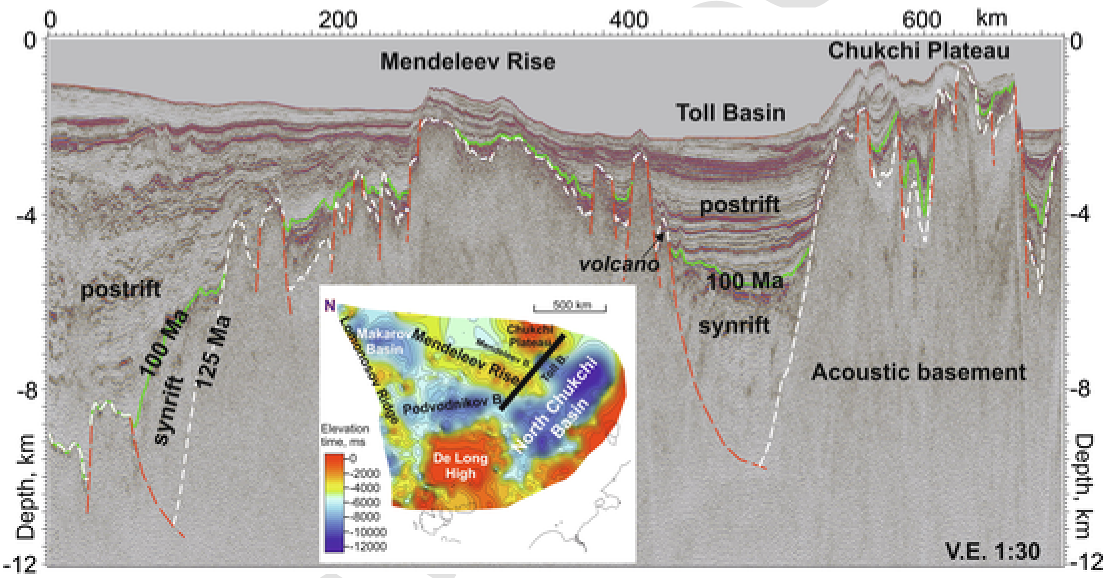

Fig. 11. Depth converted seismic line Ark 12–03 and its interpretation. Location of the line is shown on a basement time-depth map.

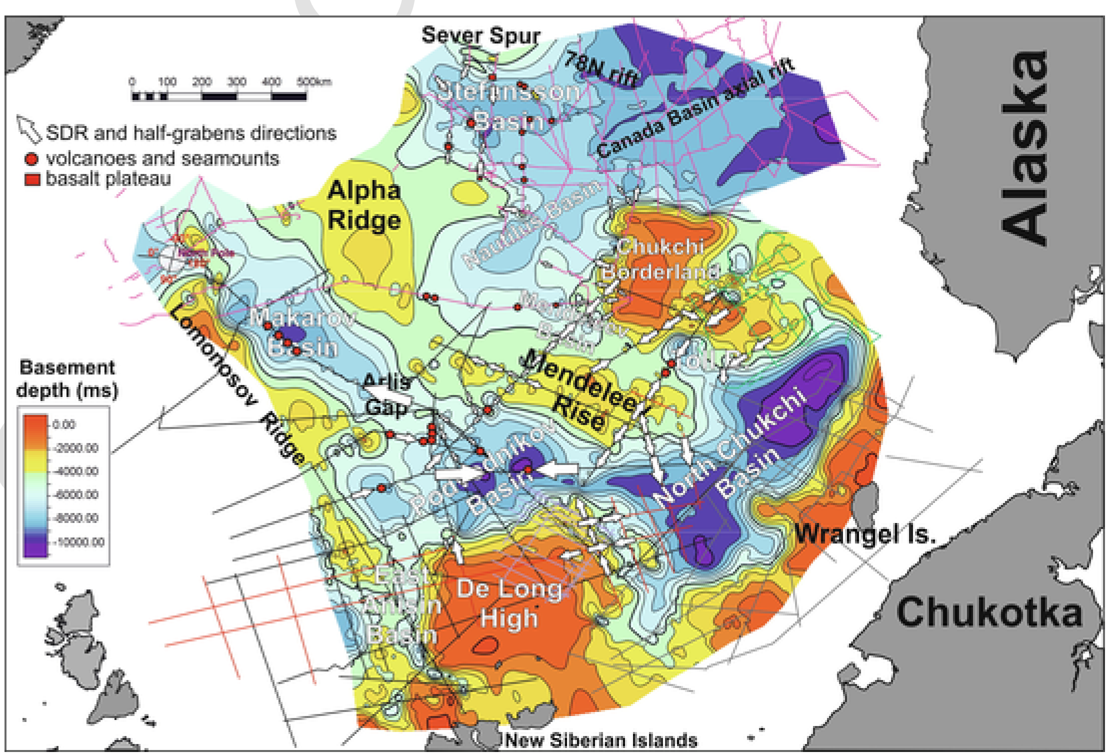

Fig. 12. Orientation of dip of reflections within half-grabens along 2D seismic lines. Length of arrow indicates length of reflector.

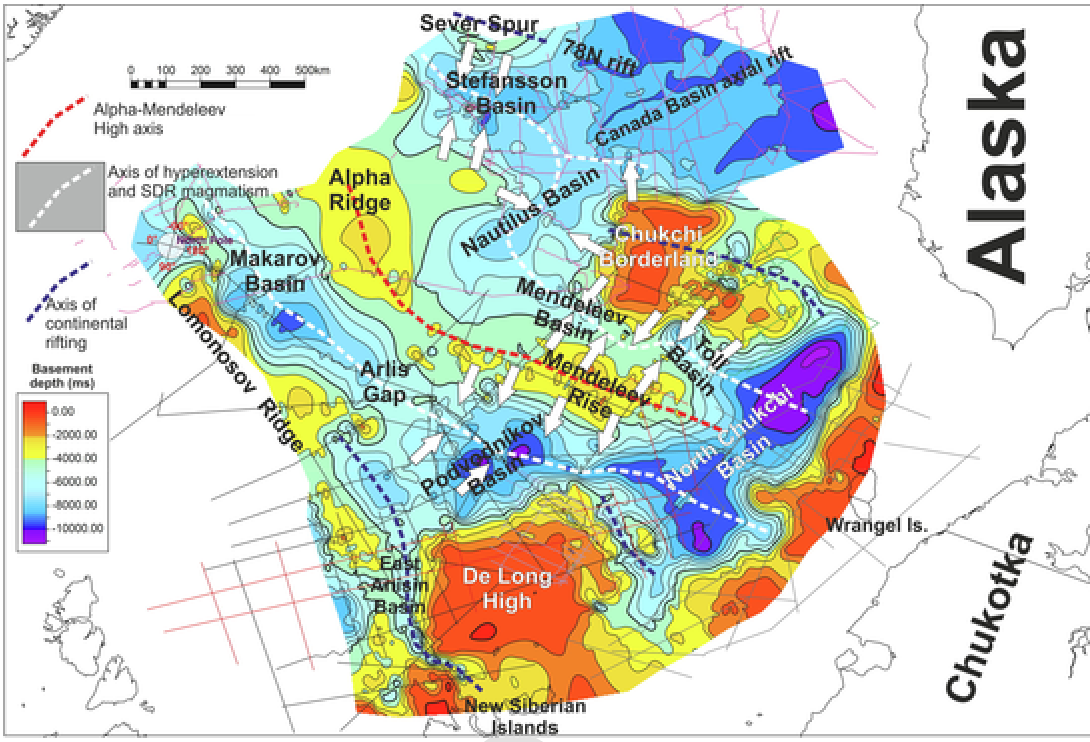

Fig. 13. Proposed orientation of dip of reflections within half-grabens (arrows). Axes of main tectonic units are shown.

identified an axial line of symmetry from which reflections dip on one slope toward the Podvodnikov Basin and on the other toward the Toll-Mendeleev basin; (2) for the Toll Basin, reflections dip toward the basin axis from the sides of the Mendeleev Rise and the Chukchi Plateau; (3) for the Podvodnikov Basin, reflections dip primarily towards its axis with a sub-meridional strike; (4) in the Podvodnikov Basin, an axial horst is outlined toward which reflections dip in the western and eastern parts of the Basin; (5) for the Stefansson Basin reflections dip primarily toward its axis; (6) in the Stefansson Basin an axial horst is proposed toward which reflections dip from both sides of the basin; (7) in the area of the Lomonosov Ridge, a complex pattern of reflection dips is observed, though in the basin of the Lomonosov Terrace reflections dipping toward the Podvodnikov Basin prevail.

In the northern part of the Toll Bain (the Mendeleev Basin), an axial V-shaped trough that cuts into acoustic basement is identified on two seismic lines (Supplementary Fig. S12). Along this part of the Toll (Mendeleev) Basin, a bright linear negative magnetic anomaly is identified by Gaina et al. (2011). We suggest that this magnetic anomaly coincides with the V-shaped trough. A present-day erosional channel is identified above the trough. Grantz et al. (1998) and Petrov and Smelror (2019) named the basin with this trough and channel the Charlie Basin. We subsequently name this V-shaped feature the Charlie Trough.

We identified on the seismic data many buried seamounts that appear to predominantly lie at the top of acoustic basement. Many of these are interpreted as volcanic edifices (Nikishin et al., 2021b). We identified three types of such edifices. The first comprise those associated with SDR-like units. Such probable volcanoes are embedded within the upper part of synrift deposits and have ages of ~ 125–100 Ma (Fig. 4). The second type has no clear relationship with underlying SDR-like units. These are large volcanic edifices older than 80 Ma. Such structures are typical of the southern slope of the Makarov Basin (Supplementary Fig. S6). The third type of buried seamount is younger (~66–56 Ma) and these lie in the area of the Lomonosov Ridge and probably the Makarov Basin (Nikishin et al., 2021b).

We compiled a thickness map of the synrift complex for the region of the AMR (Supplementary Fig. S13). Seismic data are scarce at present, and the map is thus preliminary. Our primary conclusion is that the typical thickness of the synrift complex, including the SDR-like units, is 2–3 s two-way travel time (TWT).

3.5. Rock samples from the slopes of the Mendeleev Rise

In 2014 and 2016, two Russian deep-sea geological expeditions were conducted in the region of the Mendeleev Rise. Rock sampling operations from four seamount slopes within the Mendeleev Rise were performed with the use of special deep-sea vehicles. Descriptions of these expeditions, results, and the main conclusions of these expeditions (Skolotnev et al., 2019, 2022; Nikishin et al., 2021a) are: (1) three of the seamounts > 500 km apart have a similar geological character; the lower parts of the slopes are Late Ordovician to Late Devonian deposits in the form of shelf carbonate and clastic sediments. At the seamount tops, rocks are Early Cretaceous sandstones, lavas and tuffs; (2) Paleozoic deposits, which appear on seismic lines to be within acoustic basement are pierced by many Early Cretaceous basaltic and gabbro intrusions; (3) slopes of seamounts are formed by normal faults younger than 45 Ma and landslides are common. Faults and landslides complicate restoration of initial provenance of the collected rock samples.

Isotopic ages of basaltic lavas and intrusions are 100–126 Ma with a maximum of ~ 110–114 Ma (Skolotnev et al., in preparation; Nikishin et al., 2021a). The Cretaceous lavas commonly have high porosity. Volcanic tuffs with associated clasts of sedimentary rocks were also observed. One volcanic bomb was studied and yielded a 40Ar/39Ar age of 117.3 ± 2.0 Ma (Fig. 14). This suggests that during the Aptian-Albian, volcanic islands formed (Skolotnev et al., 2022; Nikishin et al., 2021a). Preliminary analyses show that magmatic rocks have compositions from basalts and trachyte basalts to trachyte andesites. All studied rocks formed by melting in the subcontinental lithospheric mantle (Skolotnev et al., in preparation). The Cretaceous sandstones were deposited in a shallow-marine environment and dated as Barremian-Aptian age using

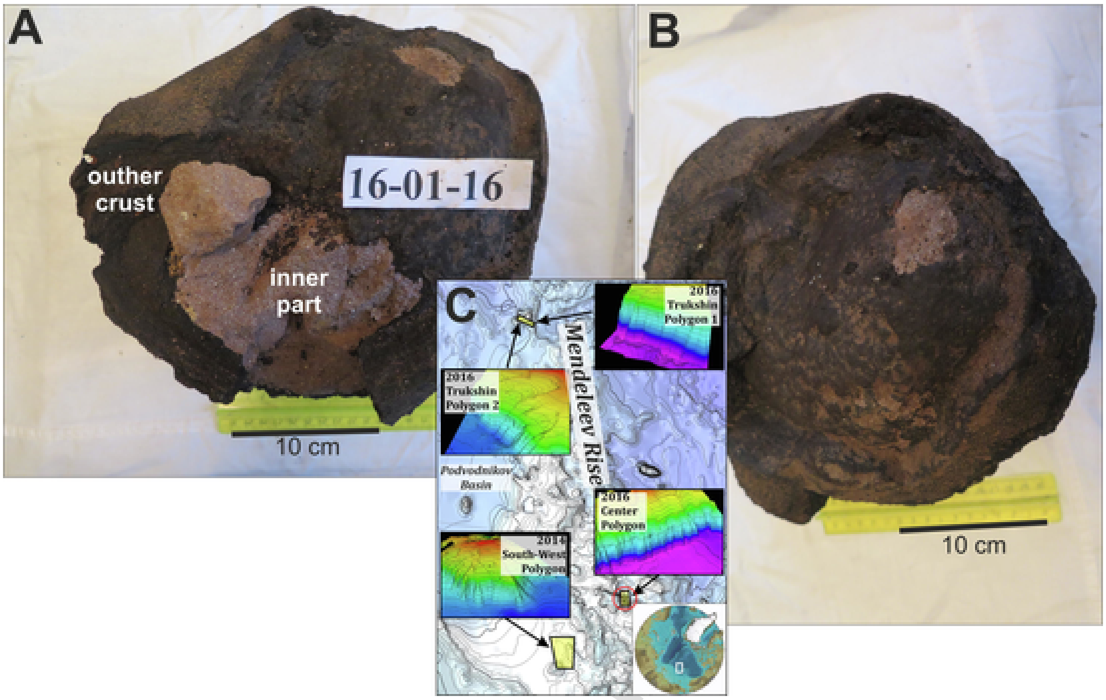

Fig. 14. Photo of volcanic bomb from two different sides (A, B) (sample 1601/16). The bomb was collected in 2016 from the Center polygon in the Mendeleev Rise (see map for location, red circle, 79° 01.3′ N, 174° 53.3′ W, water depth 1960 m) using special submarine equipment (Skolotnev et al., 2019; Nikishin et al., 2021a). It is composed of basaltic trachyandesite with 40Ar/39Ar age 117.3 ± 2.0 Ma (Skolotnev et al., in preparation). Photos by Skolotnev. (For interpretation of the references to colour in this figure legend, the reader is referred to the web version of this article.)

palynological data (Skolotnev et al., 2019, 2022). These sandstones also contain detrital zircons dated at ~ 120 Ma (Skolotnev et al., in preparation).

In the course of the Russian deep-sea expedition to the Mendeleev Rise in 2012, breccias of trachybasalts were sampled on the slopes of the Trukshin Seamount. The results of that expedition were presented by Morozov et al. (2013), Petrov et al. (2016), Kossovaya et al. (2018), Nikishin et al. (2021a). In these trachybasalts, one zircon was dated at 127.5 ± 2.7 Ma (Morozov et al., 2013).

Mukasa et al. (2020) presented a detailed description of basalts dredged on two steep submarine slopes north of the Chukchi Borderland. The samples discussed there (HLY0805-DR6 and DR7) were collected from steep escarpments with slopes up to 50° in water depths over 3500 m. They obtained three groups of 40Ar/39Ar ages: 118–112, 105–100 and 90–70 Ma. At first, low-Ti tholeiite I was formed, followed by low-Ti tholeiite II. Lastly, high-Ti tholeiites were formed. Mukasa et al. (2020) concluded that composition-time relationships for the lavas suggest melting initiation within the subcontinental lithospheric mantle.

Dredge sample HLY0805-DR1 from the Alpha Ridge yielded monolithologic outcrop samples of silicic volcaniclastic sedimentary rocks interpreted as having been deposited during a phreatomagmatic eruption (Brumley, 2014). Van Wagoner et al. (1986) and Jokat et al. (2013) previously reported recovery of acoustic basement materials in the AMR area, but these included sedimentary rocks and only a few small basalt samples. None were definitively from outcrop (Mukasa et al., 2020).

Williamson et al. (2019) reported that in August 2016, Canada's Extended Continental Margin-United Nations Convention on the Law of the Sea Program dredged approximately 100 kg of volcanic rocks from the Alpha Ridge. The dredge sample is a lapilli tuff that contains vitric and basaltic clasts. Textural evidence and the coexistence of juvenile and cognate clasts suggest a phreatomagmatic eruption. Major and trace element analyses of glassy cores indicate remarkably uniform, mildly alkaline basaltic compositions. The plagioclase-bearing glass yielded a 40Ar/39Ar plateau age of 90.40 ± 0.26 Ma.

During the 1983 CESAR expedition, many samples were dredged from the Alpha Ridge (Mudie et al., 1986; Van Wagoner et al. 1986). The oldest sedimentary rocks have Campanian to Maastrichtian microfossil ages. The deposits are biosiliceous ooze and black organic-rich mud (Mudie et al., 1986; Firth and Clark, 1998).

3.6. Gravity/magnetic crustal modelling for two regional seismic lines

Gravity and magnetic modelling was performed for seismic line 1203 (Model 1), crossing the southern parts of the Mendeleev Rise, the Toll Basin and the western Chukchi Borderland, and a composite profile composed of multi-channel seismic (MCS) lines ARC-028, 053, 065 and ARC-1204 (Model 2). These stretch from the Eurasia Basin, across the Podvodnikov Basin and northern Mendeleev Rise to the northern Chukchi Borderland. Modelling was done using GM-SYS, a 2D extension of the Geosoft Oasis Montaj software. The goal was to investigate the possible presence of a HALIP-related rock layer beneath the postrift sediments along selected seismic lines. The results are shown in Fig. 15 and Supplementary Fig. S14.

The starting structure for Model 1 was based on results from the seismo-stratigraphic interpretation of MCS data and the seismic velocity model along the "Arctika-2012" line (Kashubin et al., 2018). The starting structure for Model 2 was based on interpretations of the multichannel seismic lines listed above and Moho geometry from a regional model (Glebovsky et al., 2013). The basic petrophysical rock properties required for modelling include density, magnetic susceptibility, and remnant magnetization. Rock densities (ρ) for model blocks were calculated from seismic velocities ($\mathbf{V_p}$) obtained from refraction experiments in the Arctic Ocean (*e.g.*, Chian & Lebedeva-Ivanova, 2015; Kashubin et al., 2018; Lebedeva-Ivanova et al., 2006, 2010). The seismic results were combined to estimate average densities for model layers or blocks using functional relationships for sedimentary rocks (Gardner et al., 1974) and consolidated crustal rocks (Brocher, 2005).

Because the magnetic properties of rocks in the Amerasia Basin have not been studied, a value of 0 A/m was used for remnant magnetization

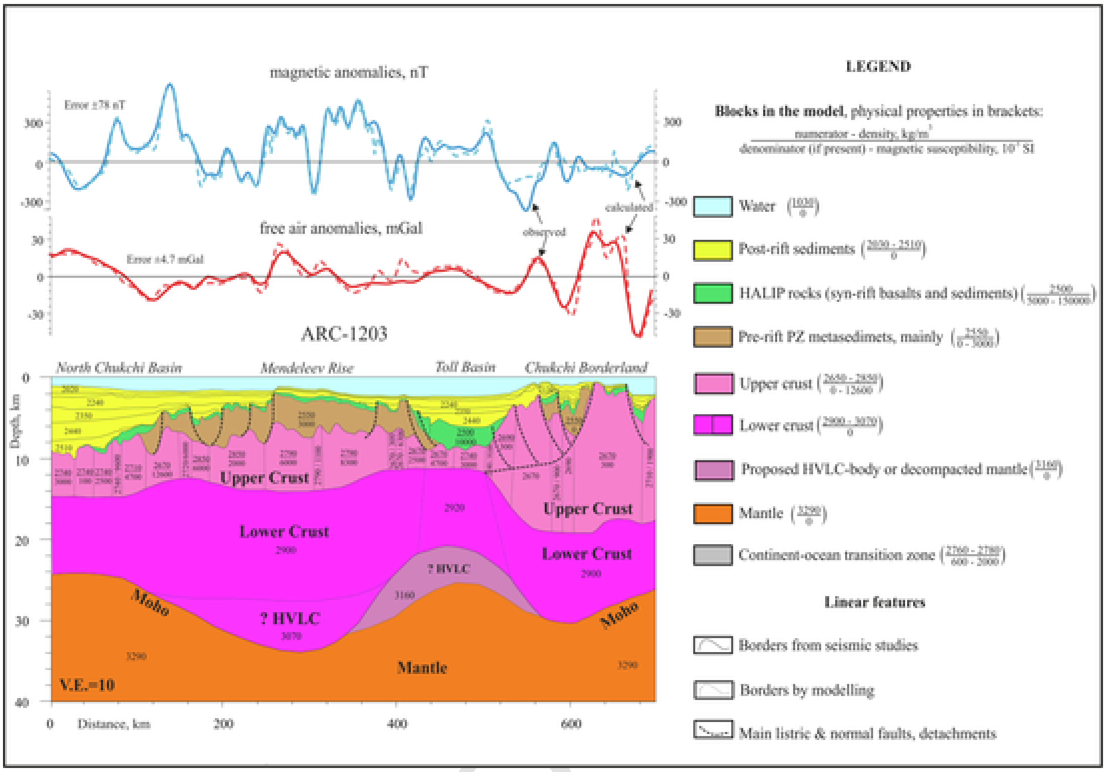

Fig. 15. Two-dimensional gravity/magnetic Model 1. The observed magnetic anomaly (solid blue graph) extracted from a grid is compared to the calculated (dashed blue line). The observed Free-Air gravity anomaly (solid red graph) extracted from a grid is compared to the calculated gravity (dashed red line). Location of Model 1 line is shown in Figs. 1 and 11. (For interpretation of the references to colour in this figure legend, the reader is referred to the web version of this article.)

and values corresponding to general petrophysical properties were used for magnetic susceptibility (χ). Ranges of modelled petrophysical properties are given in the legend of Fig. 28. The observed gravity curve was sampled from the DTU-15 satellite gravity grid (Andersen et al., 2017) and the observed magnetic curve from the magnetic anomaly grid (Piskarev et al., 2019). Modelling was conducted by iterating best-guess starting models until the observed and calculated gravity/magnetic curves matched. Some misfits in amplitudes of the observed and calculated gravity curves (significant in Model 2, at the Lomonosov Ridge) arise from the smoothed character of the former, extracted from the grid (see Fig. 16).

The shallowest layer comprises postrift sediments. These rocks are non-magnetic and have densities in the range 2030–2510 kg/m^3 (V_p = 1.8–5.0 km/s). They overlie the layer of synrift HALIP rocks suggested by studies of magnetic anomalies (*e.g.,* Grantz et al., 2011a,b; Saltus et al, 2011; Oakey and Saltus, 2016) and dredging and sampling in the deep Arctic Ocean (*e.g.,* Andronikov et al. 2008; Brumley et al., 2015; Jokat et al., 1999; Skolotnev et al., 2019). We model the upper part of this layer (V_p = 4.0–4.5 km/s) using MCS data, which provided evidence for volcano-sedimentary sequences including dipping reflections and SDRs (*e.g.,* Bruvoll et al., 2011; Nikishin et al., 2021b). The depth to the base of this layer is speculative and inferred using joint gravity/magnetic modelling. In our models the thickness of the *syn*-rift volcano-sedimentary layer ranges from 150 to 200 m over the highs to 3000 m over the basins. While Vp is 4.0–4.5 km/s at the top of the layer, the average density used is 2500 kg/m^3 and constant.

Magnetic susceptibilities spanning the wide range of 5000–150,000SI were used. Our magnetic modeling is speculative since it is constrained only by observations at the top. Nevertheless, models support the existence of a *syn*-rift HALIP layer with typical petrophysical properties in areas where high-amplitude, highly variable magnetic anomaly fields are observed.

A *meta*-sedimentary layer exists in the structure of high-standing crustal blocks in the Amerasia Basin and frequently underlies the HALIP layer. It comprises pre-rift Paleozoic rocks beneath the Mendeleev Rise (Skolotnev et al., 2019) and the Chukchi Borderland (*e.g.,* Grantz et al, 1998). This layer is detected by refraction data only (*e.g.,* Poselov et al., 2011; Kashubin et al., 2018) and has a V_p = 4.5–5.4 km/s and thickness up to 4.5 km. It is thought to be absent beneath the basins because of dramatic reworking during continental rifting. We assigned a density of ρ = 2550 kg/m^3 and magnetic susceptibility χ = 3000SI due to the possibility of frequent magmatic intrusions in this layer.

The existence of other crustal layers is inferred from refraction seismic data (*e.g.,* Poselov et al., 2011; Evangelatos et al., 2017). Their thickness variations along the models are determined by gravity modelling. The upper crust is represented by a layer 8–18 km thick at the highs, thinning to ~ 3 km under the basins. Density varies in the range 2650–2850 kg/m^3 (V_p = 5.8–6.7 km/s) and χ = 0–12600SI. The Mendeleev Rise is characterized by an ~ 8 km thick upper crust and high/maximal values of ρ and χ. The latter is likely due to numerous magmatic intrusions. The lower crust has a minimal thickness of ~ 10 km under the basins and a maximum thickness of ~ 20 km beneath the highs and the Mendeleev Rise in particular. The average ρ was set to 2900–2920 kg/m^3. In Model 1 a dense (ρ = 3070 kg/m^3), high-velocity lower crust (HVLC) block (V_p = 7.3 km/s) is placed at the base of the lower crust based on seismic data (Kashubin et al., 2018).

The same block is speculatively introduced into Model 2 on the basis of seismic results from Jackson & Chian (2019) and Lebedeva-Ivanova et al. (2006, 2010). The lithospheric mantle is assigned a density of ρ = 3290 kg/m^3 (V_p = 8.0 km/s), decreasing beneath the Toll Basin to 3160 kg/m^3 with V_p = 7.8 km/s based on results of Kashubin et al. (2018). We speculate that this decrease could be explained by a HVLC-block rather than decompacted mantle.

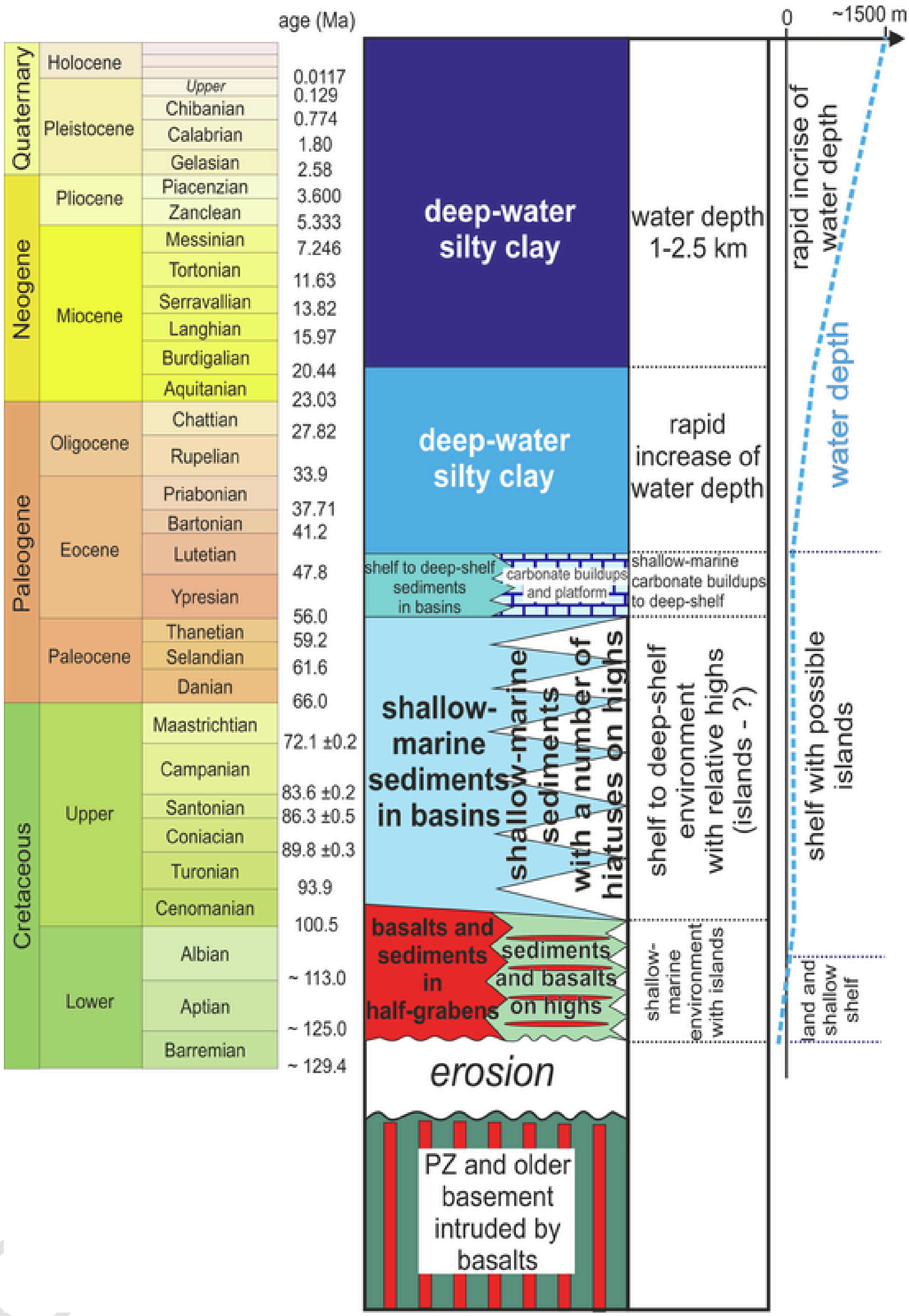

Fig. 16. Chronostratigraphy of the Mendeleev Rise.

4. Results

4.1. Correlation of events for the Mendeleev Rise and the Podvodnikov, Toll, Makarov and North Chukchi basins

For the AMR and the Podvodnikov, Stefansson, North Chukchi and Toll basins, we discriminated between synrift and postrift deposits (Figs. 4, 5, 6, 7, 8). Seismic profiles show with high probability that the rift-postrift boundary for these structures is approximately coeval. That is, there is no evidence to support a succession of events responsible for the formation of the Mendeleev Rise and adjoining deep-sea basins. The Mendeleev Rise constituted a mid-basinal high and the adjoining Podvodnikov and Toll basins formed as deep-sea basins quasi-symmetrical with the axial zone of the Mendeleev Rise (Nikishin et al., 2021b). We propose the same for the Alpha Ridge and Stefansson Basin. In our seismo-stratigraphic model, the rift-postrift boundary for the basins of the East Siberian Sea dates to ~ 100 Ma. In the Mendeleev Rise area, it might be the same or possibly somewhat younger, *e.g.*, 90 Ma (Nikishin et al., 2021b).

The southernmost part of the Mendeleev Rise extends into the North Chukchi Basin as the Kucherov High, dividing the basin into the West and East North Chukchi Basins. The Kucherov High in the North Chukchi Basin is characterized by a gentle acoustic basement uplift. On its slopes are systematically onlapping seismic reflections. The uplift is directly overlain by seismic complexes aged ~ 90–100 Ma (Supplementary Figs. S4 and S5).

The rift-postrift boundary at the top of the SDRs on the Mendeleev Rise may be synchronous with the rift-postrift boundary within the North Chukchi Basin (Fig. 5 and Supplementary Figs. S4, S7, S8). Unfortunately, our seismic data are insufficient to adequately address this complex relationship. However, we infer that the synrift deposits in the North Chukchi Basin experienced significant extension and became a part of the acoustic basement. It is also possible that the postrift deposits of the North Chukchi Basin overlie directly exhumed lower crust complexes as proposed by Nikishin et al. (2021b). A general correlation of events suggests that the Kucherov High (the southern continuation of the Mendeleev Rise) formed synchronously with hyper-extension of the continental crust of the North Chukchi Basin.

Our correlations of seismic lines indicate that it is likely that formation of the Mendeleev Rise and the adjoining Podvodnikov, Toll, and North Chukchi basins took place synchronously in a single geodynamic system starting at ~ 125 Ma and ending at 100–90 Ma. In the deep-water part of the ocean, rifting might have terminated later (circa 90 Ma) (see also Nikishin et al., 2021b). We propose the same for the Alpha Ridge and Stefansson Basin.

Our seismo-stratigraphic correlation between the Podvodnikov and Makarov basins is difficult for now, given the limited areal coverage of 2D seismic lines. Nonetheless, Nikishin et al. (2021b,c) observed that the Makarov Basin likely also had younger phases of rifting in the Late Cretaceous – Early Cenozoic.

4.2. SDR-like seismic units and half-grabens

SDR-like seismic units and half-grabens are prominent in the AMR and the Podvodnikov, Stefansson, and Toll basins. For the Mendeleev Rise, we can confidently draw an axial line along the rise, separating probable half-grabens of different polarity. On the western slope, all bright reflections are characterized by westward dips (normal faults of half-grabens have eastward dips), while on the eastern slope of the Rise, all bright reflections are characterized by eastward dips (normal faults of half-grabens have westward dips). From the available data it is clear that the Mendeleev Rise is a symmetrical structure, complicated by Cenozoic faults as discussed by Nikishin et al. (2021b,c).

In the Podvodnikov Basin, bright reflections in the eastern part dip mainly westward toward the center of the basin while in the western part reflections dip mainly eastward. We have insufficient data to fully understand the structure of the Podvodnikov Basin. At its center there is an axial horst-like uplift of acoustic basement, which extends approximately parallel to the Mendeleev Rise. This uplift is considered to be the Axial Tectonic High.

In the southern part of the Toll Basin, the situation is similar to that in the Podvodnikov Basin. Distinct SDR-like units dip from the Chukchi Plateau side toward the axial part of the basin. Reflections on the eastern slope of the Mendeleev Rise also dip toward the axis of the Toll Basin. For the Makarov Basin we have, as yet, not identified SDR-like units. The Stefansson Basin is very similar to the Podvodnikov Basin in general.

4.3. Geological data relating to Alpha-Mendeleev Rise formation history

For the Mendeleev Rise, we have seismic lines and rock samples from the slopes. Rifting with associated accumulation of clastic sediments started in the Aptian when the sea was shallow as suggested by lithology of the sandstones (Skolotnev et al., 2022) and by Paleocene shallow-water carbonate buildups (Posamentier et al., in preparation). Approximately synchronous with the start of rifting circa ± 125 Ma, basaltic volcanism characterized primarily by increased-alkalinity basalts and andesites began. Volcanism continued until 100–110 Ma, a time when the Mendeleev Rise remained shallow-marine and locally subaerial as shown by the volcanic bombs and tuffs observed there. Thus, Mendeleev Rise Aptian-Albian paleogeography likely was that of a strip of shallow shelf sea with volcanic islands.

Dredged lapilli tuff containing vitric and basaltic clasts constrain Cretaceous magmatism on the Alpha Ridge. A 40Ar/39Ar plateau age of these rocks yields 90.40 ± 0.26 Ma (Williamson et al., 2019). Possible felsic volcanic centers were proposed by Brumley (2014) using seismic data. Shimeld et al. (2019) and Funck et al. (2022) reported that coincident seismic reflection and refraction data collected during the 2016 Canada-Sweden Polar Expedition across the northern and southern flanks of the Alpha Ridge reveal a range of igneous phenomena, and allow preliminary identification of important tectono-magmatic elements. Igneous intrusions on the northern periphery of the Alpha Ridge are broadly parallel to both the Marvin Spur and the CESAR valley, suggesting that the tectonic fabric affected magma delivery conduits. Positive bathymetric features on the ridge, such as the Fedotov Seamount, exhibit acoustic facies interpreted as stacked effusive volcanic sequences emanating from discrete volcanic centers (Shimeld et al., 2019).

Data on magmatism for the AMR suggest two phases of such magmatism: (1) 125–90(?) Ma half-grabens with basalts, SDR-like units and individual volcanoes formed; (2) circa 90–80 Ma individual volcanic centers formed after the main formation of the AMR.

Rock dredging on the Alpha Ridge shows that Campanian-Maastrichtian deposits comprise biosiliceous ooze and black organic-rich mud (Mudie et al., 1986; Firth and Clark, 1998). They could have formed on a relatively deep shelf. Seismic data show that sediments of ~ 100–56 Ma in the form of a thin layer probably draped parts of the Mendeleev Rise. Bathymetric lows contain shallow-marine sediments, and highs show hiatuses. Sediments of 56–45 Ma age drape most of the Mendeleev Rise. Relative lows have shelf to deep-shelf sediments including mass transport deposits (MTDs). Relative highs have possible carbonate deposits including carbonate buildups (Posamentier et al., in preparation). Sediments of 45–20 Ma drape most of the Rise. This was a time of rapid increase of water depth. During 45–20 Ma vertical movements with normal faulting occurred (Supplementary Fig. S3) (Nikishin et al., 2021b,c) followed by an erosional event at ~ 20 Ma (Nikishin et al., 2021b,c). Deep-water 20–0 Ma deposits cover the entire Mendeleev Rise with nearly uniform thickness. A tectonostratigraphic chart for the Mendeleev Rise is shown in Fig. 30. The southern slope of the Alpha Ridge was affected by an additional normal faulting phase during the Late Cretaceous at ~ 80–66 Ma.

4.4. Geological data concerning the formation history of the Podvodnikov and Makarov basins

For the Podvodnikov Basin and the adjoining Lomonosov Terrace Basin, a synrift complex is identified with possible SDR-like units. Nikishin et al. (2021a) presented a seismic velocity model along the same seismic sections based on seismic refraction measurements made using sonobuoys. This model suggests basalts within the synrift deposits. At the center of the basin, the Axial Tectonic High was identified. At the top of the section containing the SDR units buried seamounts interpreted as volcanoes were observed (Nikishin et al., 2021b). These volcanoes show no evidence of subaerial erosion and probably were subaqueous. Their heights reach 0.6 s TWT. Thus, by the end of the rifting epoch, ocean depths in the Podvodnikov Basin reached 0.5–1 km. Seismic data and clinoforms of the North Chukchi Basin suggest that distal turbidite facies formed in the Podvodnikov Basin during the Paleocene and that the basin was a deep-water depositional environment.

For the Makarov Basin, no SDR-like units have so far been observed. The rift-postrift boundary is not distinctly identifiable. In synrift deposits or at their top, many volcanic edifices are outlined up to 1.2 s TWT high with no evidence of erosion. This suggests that by the end of rifting the paleo-water depth of the marine basin was > 1 km.

4.5. Geological data concerning formation history of the Toll and Mendeleev basins

For the Toll Basin, distinct SDR-like units are identified on both the Russian and American seismic data (Nikishin et al., 2014, 2021a,b; Ilhan and Coakley, 2018). At the top of the SDR-like units there are probable subsea volcanoes up to 0.5 s TWT high. Thus, by the end of rifting, the marine basin was at least 0.5–0.8 km deep. In the north the Toll basin transitions to the Mendeleev Basin via the axial Charlie Trough (Fig. 19). The Charlie Trough is symmetrical with no indications of synrift segmentation. Nikishin et al. (2021b) proposed that the Charlie Trough represents an aborted phase of disruption of continental lithosphere and can be considered a failed oceanic rift.

4.6. Geological data concerning the formation history of the Stefansson Basin

The Stefansson Basin is very similar to the Podvodnikov Basin. It has symmetric SDR-like seismic units along both slopes and possibly an axial basement high. The basin was affected by additional normal faulting during the Late Cretaceous (approximately 80–66 Ma). This extensional phase affected the Sever Spur slope according to our preliminary correlation of the seismic data.

5. Discussion

5.1. What are the SDR-like seismic units?

In passive continental margins, Inner SDRs and Outer SDRs are distinguished (*e.g.*, Stica et al., 2014; Geoffroy et al., 2015; Paton et al., 2017; Guan et al., 2019; Harkin et al., 2020; Chauvet et al., 2021). Inner SDRs are formed in half-grabens on continental crust synchronously with continental rifting. The type of crust on which Outer SDRs are formed is under discussion (*e.g.*, Mutter, 1985; Geoffroy et al., 2015; Buck, 2017; Paton et al., 2017; Norcliffe et al., 2018; Foulger et al., 2020; Harkin et al., 2020; Lang et al., 2020; Chauvet et al., 2021). Inner- and Outer SDRs on continental margins often form continuous series (*e.g.*, McDermott et al., 2018, 2019). In some instances, between Inner- and Outer SDRs, an outer high is identified in the form of volcanoes (*e.g.*, Planke et al., 2020).

For the AMR SDR-like seismic units form wedges separated by highs which likely comprise basement uplifts. We have no evidence that these highs are volcanic edifices. Nonetheless, based on our observations, we conclude that alternating half-grabens and basement horsts characterize the AMR and that the half-grabens formed nearly synchronously. The half-grabens are filled with volcanics and possible associated sediments. The geological structure of the Rise is similar to the Inner SDR zone of volcanic passive continental margins. In the Podvodnikov Basin, the geometry of SDR-like units is similar to Inner- and Intermediate SDRs in the classification of Chauvet et al. (2021).

5.2. Major structures formed in the Aptian-Albian

Fig. 17 shows a map of major Aptian-Albian structures (see also Figs. 12 and 13). For the Mendeleev Rise (and possibly the entire AMR) an axial line is identified that separates slopes of the Rise with differently-oriented reflection dips in the half-grabens. On the eastern slope reflections dip eastward while on the western slope they dip westward. The AMR can be considered a double-sided continental volcanic passive margin.

For the Podvodnikov and Toll basins, reflections in the synrift complexes dip toward the axial parts of the basins. Axial highs represent uplifted basement blocks. Because of limited seismic coverage we cannot as yet precisely contour these blocks. In the Mendeleev Basin we identify the Charlie Trough, which we interpret as a failed oceanic rift. The Podvodnikov and Toll-Mendeleev basins likely comprise failed oceanic basins.

In the Stefansson Basin reflections in the synrift complexes dip toward the axial part where we propose a basement high. The North Chukchi Basin is divided into two parts. The western part is a continuation of the Podvodnikov Basin and the eastern part is a continuation of the Toll Basin. During its formation the extension axis in the North Chukchi Basin ran approximately north–south. In the Aptian-Albian, it was a relatively deep-water basin with a paleogeography similar to that of the Podvodnikov and Toll Basins.

5.3. Crustal structure of the Alpha-Mendeleev Rise and adjoining deep-water basins

There are several models for the crustal structure of the AMR based on German and American seismic data (*e.g.*, Weber, 1986; Jackson et al., 1986; Jokat, 2003; Funck et al., 2011; Bruvoll et al., 2012; Jokat and Ickrath, 2015). According to these models, the AMR comprises thickened oceanic crust of basaltic composition. As new geophysical data have become available, proposed models have emphasised the role of continental crust (*e.g.*, Oakey and Saltus, 2016; Jackson and Chian, 2019). Several crustal structure models based on Russian seismic data have been presented by Lebedeva-Ivanova et al. (2006, 2011, 2019), Chernykh et al. (2016), Kashubin et al. (2018), Piskarev et al. (2019), and Nikishin et al., 2021a. These models propose continental crust beneath the Mendeleev Rise and the Podvodnikov Basin. Lebedeva-Ivanova et al. (2019) reviewed available seismic data and showed that high-velocity lower crustal bodies (HVLCB) are present within the lower crust of the AMR and the Podvodnikov Basin. Integrating the models of Lebedeva-Ivanova et al. (2006, 2019), Chernykh et al. (2016) and Kashubin et al. (2018) with our geophysical data (Fig. 15), we propose a tectono-stratigraphic architecture between the Lomonosov Ridge and the Chukchi Plateau in Fig. 18.

Rock sampling data from the slopes of the Mendeleev Rise (Skolotnev et al., 2019, 2022) show that its basement is extensively associated with basaltic intrusions. This is a common feature of Inner SDRs, and consistent with observations from Greenland (*e.g.*, Geoffroy, 2005; Abdelmalak et al., 2015). We interpret the crust of the Mendeleev Rise to be similar to the Inner SDRs of volcanic margins.

The crust beneath the Podvodnikov and Toll basins is probably also continental., though likely hyper-extended. Three observations support this hypothesis: (1) a HVLC body, which suggests saturation of the lower crust with basaltic intrusions; (2) SDR-like units; and (3) Axial Tectonic Highs, which are likely continental crustal basement uplifts.

The crust of the North Chukchi Basin most probably comprises hyper-extended continental crust as supported by seismic data (Petrov and Smelror, 2019; Piskarev et al., 2019). Our seismic data show that synrift deposits are part of the acoustic basement and a system of detachments may lie at the base of the postrift deposits (Nikishin et al., 2021b).

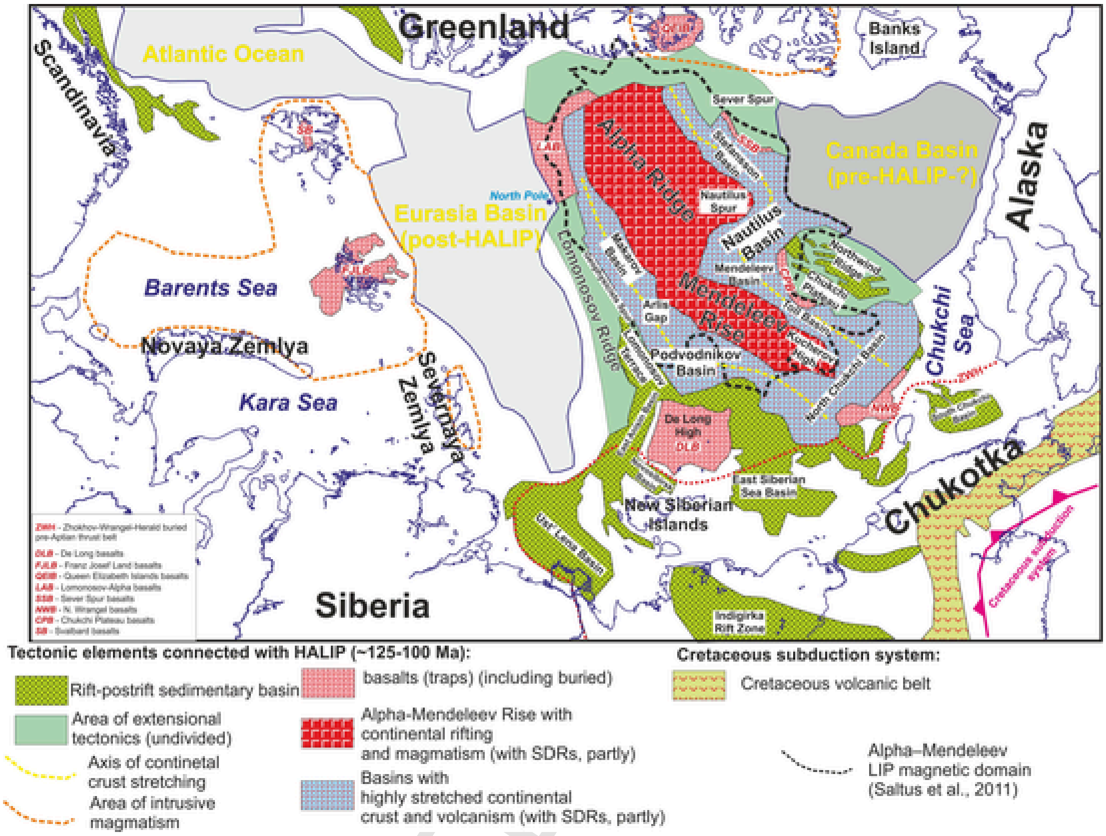

Fig. 17. Map of major Aptian-Albian structures. Outlines of Alpha-Mendeleev LIP magnetic domain are after Saltus et al. (2011).

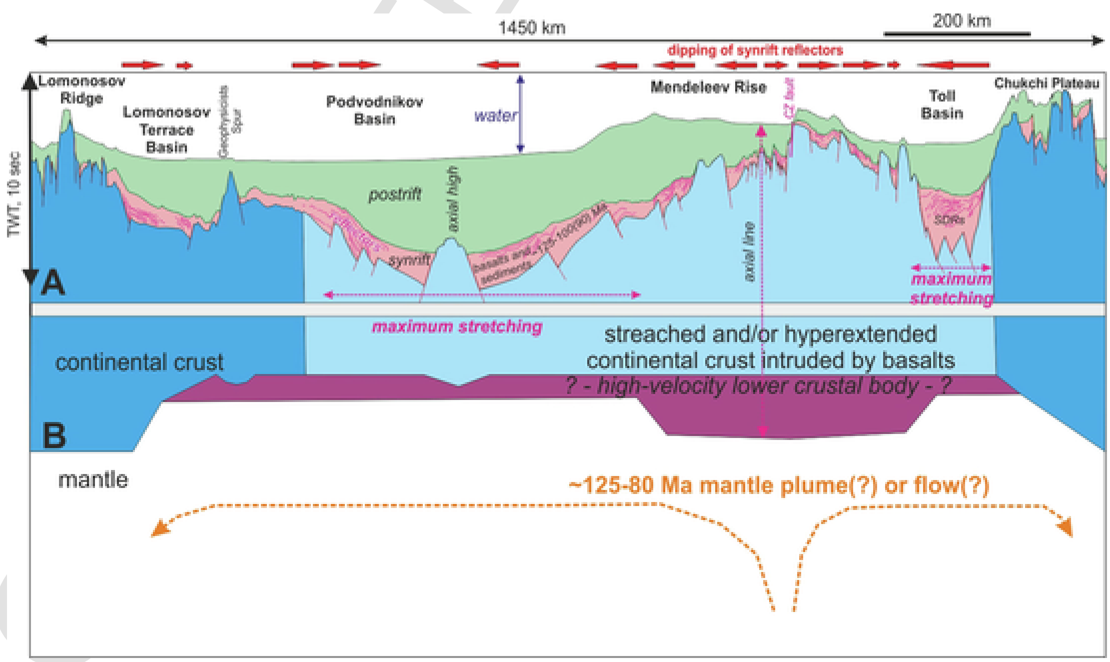

Fig. 18. Conceptual model of the crustal structure of the Mendeleev Rise and adjacent area. A. Interpretation of seismic data (Fig. 4) for the upper crust. B. model of the lower crust structure (Fig. 15).

5.4. Tectonic reconstruction of the formation of the Alpha-Mendeleev Rise

Several kinematic reconstructions of the formation history of the AMR have been presented recently (*e.g.*, Doré et al., 2015; Døssing et al., 2017; Chernykh et al., 2018; Sømme et al., 2018). The reconstructions of Døssing et al. (2017) and Chernykh et al. (2018) are based mainly on magnetic and gravity anomalies. Nikishin et al. (2021c) published a reconstruction for the Arctic for the Aptian-Albian. Proposed reconstructions vary based upon which data were used in the analyses. In our approach, we use seismic stratigraphy to correlate events from different areas of the Amerasia Basin, in conjunction with new rock sampling on slopes of the Mendeleev Rise.

Basaltic plateaus with ages of ~ 125–100 Ma are well known in the north of the Canadian Archipelago, on Spitsbergen, Franz Josef Land, and around the De Long Islands. We identified the North Wrangel Magmatic Province using seismic lines and magnetic and gravity anomalies (Nikishin et al., 2021c). This province is characterized by basaltic lavas and numerous intrusions with a seismic-stratigraphic ages of ~ 125 Ma. We propose a magmatic province of this age along the western edge of the Chukchi Plateau based on seismic lines and magnetic anomalies.

The AMR formed as a belt of continental rifting and volcanism in a shallow-water marine basin with volcanic islands. Along the edges of the AMR, two belts of relatively deep-water basins formed by hyper-extension of continental crust and subaqueous volcanism. One of these belts is the West North Chukchi, Podvodnikov and Makarov Basins. The other comprises the East North Chukchi, Toll, Mendeleev and possibly Nautilus and Stefansson Basins. At the southern extremity of the Mendeleev Rise (the Kucherov High), the North Wrangel Magmatic Province formed.

The Mendeleev Rise can be considered a mid-basinal high of the failed oceanic basin between Eurasia (the Lomonosov Ridge was a part of Eurasia) and the Chukchi Plateau continental terrane. The Alpha Ridge can be considered a mid-basinal high for the failed oceanic basin between Eurasia and the Canada Basin.

5.5. The Alpha-Mendeleev Rise and magnetic anomaly data

Saltus et al. (2011) analyzed magnetic anomalies in the Arctic Ocean. They identify the Alpha-Mendeleev region as the Alpha-Mendeleev Large Igneous Province. The outline of this proposed province is shown in Fig. 17. Oakey and Saltus (2016) describe this analysis. They distinguish the High Arctic Magnetic High Domain or HAMH. The outline of this domain is similar to outlines of the Alpha-Mendeleev Large Igneous Province of Saltus et al. (2011) (Oakey and Saltus, 2016, Fig. 2). The HAMH was interpreted as a Large Igneous Province using 2D gravity/magnetic modelling.

We added the outline of the Alpha-Mendeleev Large Igneous Province as proposed by Saltus et al. (2011) and Oakey and Saltus (2016) to our map of major tectonic and magmatic structures formed in the Aptian-Albian (Fig. 19). A key conclusion is that the HAMH domain closely coincides with our areas with SDR-like seismic units. This means that HAMH domain (or the Alpha-Mendeleev Large Igneous Province) originated during HALIP time (125–100 Ma with local prolongation up to 80 Ma) on pre-Cretaceous continental crust. We propose that this process had no connection with Canada Basin opening. We find no evidence of any earlier oceanic crust in the Alpha-Mendeleev Large Igneous Province.

5.6. The role of strike-slip faults and the Cenozoic history of the Mendeleev Rise

Døssing et al. (2017) and Chernykh et al. (2018) make wide use of strike-slip faults in their tectonic reconstruction of the AMR region. These proposed faults are mainly based on gravity and magnetic anomalies and bathymetry. While we agree that strike-slip faults likely played an important role in the formation of the AMR region, the precise depiction in terms of degree of offset and throw associated with these faults can vary widely. Up until now adequate differentiating data have been lacking.

Bruvoll et al. (2010) and Nikishin et al. (2014, 2021b,c) showed that the present-day relief of the AMR region with its horst-graben structure formed mainly by Cenozoic transtensional deformation. The lack of direct correspondence shows that present-day relief is not an indication of the Mesozoic structure of the region.

5.7. Analogues of the Alpha-Mendeleev Rise

Foulger et al. (2020) proposed a new model for the formation of the North Atlantic. They proposed that the crust beneath Iceland, and the adjacent shallow bathymetric ridges that connect it to Greenland and the Faroe Islands, contain extensive continental crust. In their model, this structure formed by hyper-extension and magma-inflation of continental mid- and lower crust. The mid-Atlantic ridge, in a complex form, has traversed this region for the entire ~ 52 Myr period of ocean opening (Geoffroy et al., 2022). The basalt magma produced at this extensional plate boundary caps the continental lower crust. A swath of parallel extinct and currently active rifts produced lavas that form dipping successions, and these are analogues to SDRs. They are exposed subaerially in Iceland itself (Foulger et al., 2020; Geoffroy et al., 2020; Foulger et al., 2022; Geoffroy et al., 2022). The known Jan Mayen Microcontinental Complex north of Iceland may be a continuation of this structure.

In this model, the entire 1200-km-long Greenland-Iceland-Faroe Ridge can be described as an unusually wide pair of volcanic passive margins. It is possible that a relatively large block of largely coherent continental crust underlies Iceland and that the unusually large width of the Ridge is a result of there being two pairs of passive volcanic margins, one on each side of the microcontinent, instead of the usual one pair.

North and south of the Greenland-Iceland-Faroe Ridge volcanic continental margins formed, including the Vøring Plateau, which is known to be underlain by continental material. HVLC is extensive along the margins and is considered by some workers to be continental in nature (*e.g.*, Guan et al., 2019; Lebedeva-Ivanova et al., 2019; Geoffroy et al., 2020; Biari et al., 2021). This hypothesis of a continental Greenland-Iceland-Faroe Ridge is supported by recent interpretations of marine seismic profiles (*e.g.*, Yuan et al., 2020). Our findings provide strong evidence that the AMR comprises a very similar structure to that proposed for the Greenland-Iceland-Faroe Ridge.

5.8. Geodynamic model of formation of the Alpha-Mendeleev Rise region

We propose the AMR and conjugate deep-water basins to be of Aptian-Albian age and to constitute a failed oceanic basin. The Rise itself is a failed mid-basinal high, while the conjugate basins are failed oceanic basins. Our tectonic reconstruction of the Arctic for Aptian-Albian time shows that the region of the AMR developed as an intraplate tectonic structure. The reconstructions presented by Shephard et al. (2013) and Døssing et al. (2020) also propose an intraplate position of the Amerasia Basin in the Aptian-Albian. It is likely that it was simply the intraplate position of the AMR that prevented formation of a fully-fledged ocean. The Pacific Ocean subduction zones were relatively far away. There may have been Cretaceous strike-slip faults connecting the Pacific Ocean subduction regime to the region of the AMR (*e.g.*, Doré et al., 2015; Nikishin et al., 2021b).

We base our conceptual geodynamic model (Fig. 20) on those of Geoffroy et al. (2015, 2020) and Foulger et al. (2020, Fig. 19). As for the Iceland region, the mantle plume model is popular for explaining the magmatism. In the case of the Arctic Ocean, the equivalent magmatism is the HALIP. Given the radical new possibility that much of the crustal material previously thought to be magmatic may, instead, be continental, the true magmatic volumes may need to be greatly downward-revised. The need to invoke mantle plumes to account for the volumes can then be re-visited.

It is unclear why the AMR region did not evolve into a fully fledged ocean. Two possible explanations are: (1) the region formed in an intraplate tectonic setting unconnected with the wider system of mid-oceanic ridges; and (2) at approximately 105–110 Ma, a global-scale plate reorganization event took place (Matthews et al., 2012) that affected geodynamics in the Arctic – a reorganization that resulted in rift-

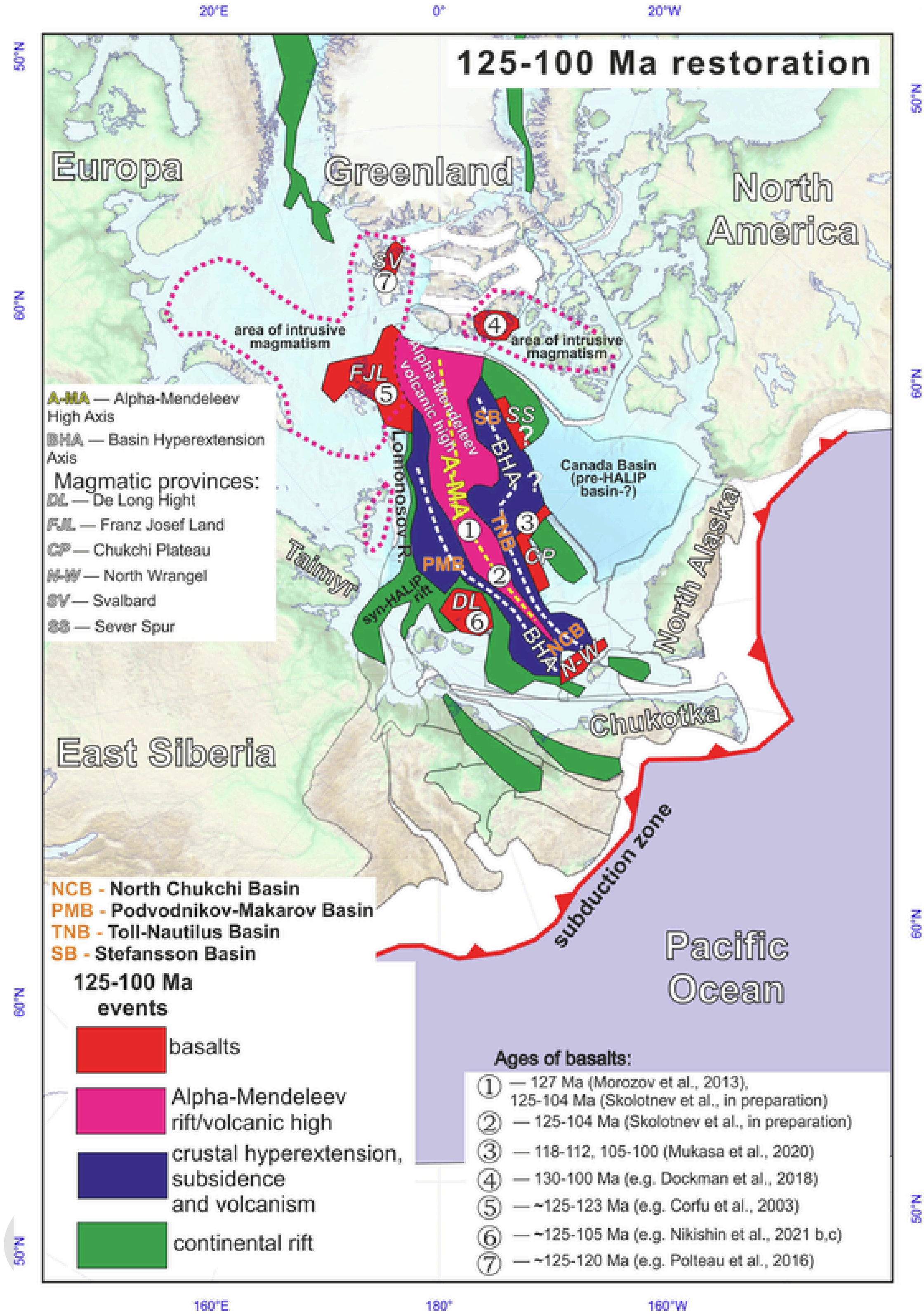

Fig. 19. Paleotectonic restoration for Aptian-Albian time. Modified after Nikishin et al. (2021c). Ages of basalts are from (Morozov et al., 2013; Mukasa et al., 2020; Dockman et al., 2018; Corfu et al., 2013; Nikishin et al., 2021b,c; Polteau et al., 2016; Skolotnev et al., in preparation).

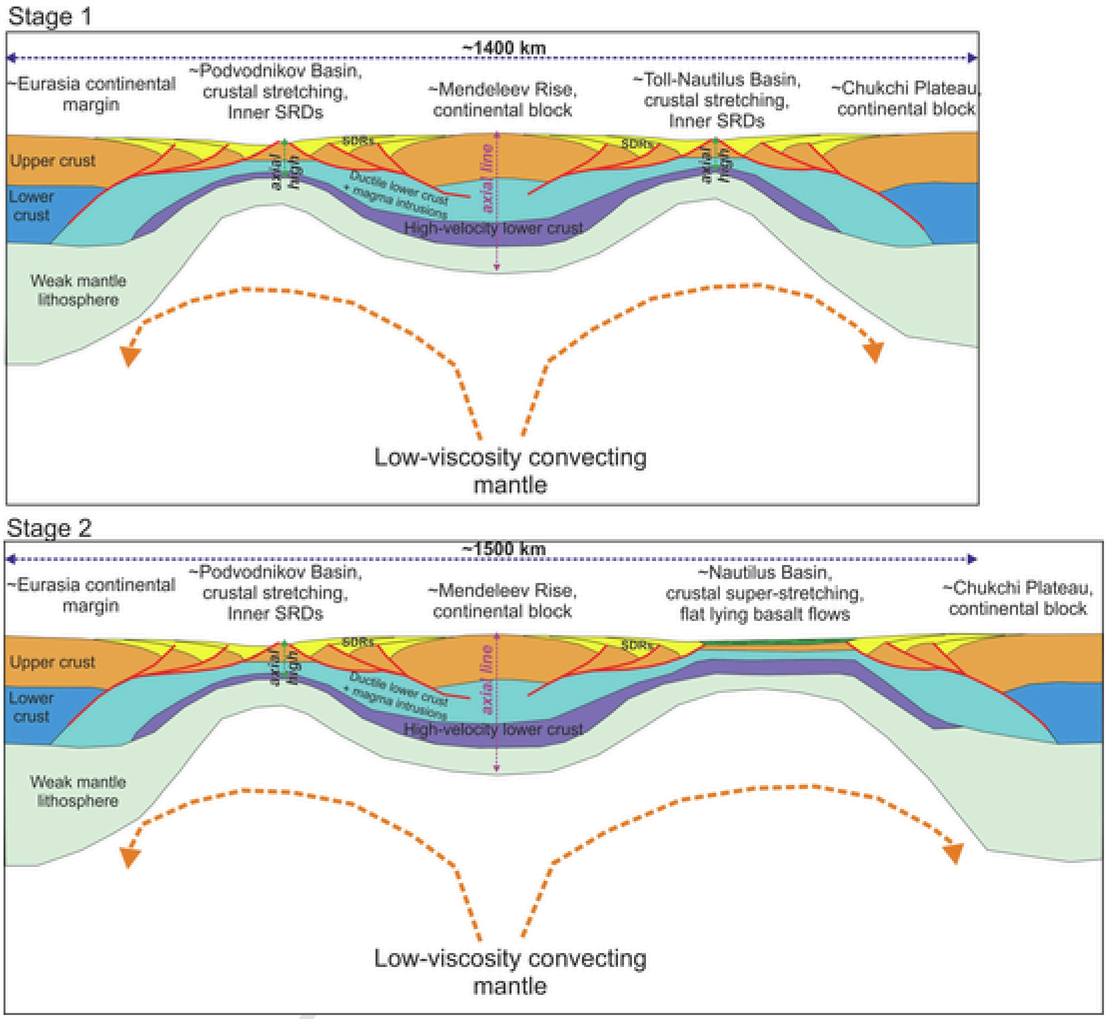

Fig. 20. Schematic geodynamic model for the Mendeleev Rise and adjacent deep-water basins for Aptian-Albian time. The models of Geoffroy et al. (2015, 2020) and Foulger et al. (2020) were used with modifications.

ing ceasing since it was no longer required (*e.g.* Ziegler and Cloetingh, 2004).

6. Conclusions

Our main conclusions are:

1. The AMR formed as a double-sided volcanic passive continental margin on continental crust in the Aptian-Albian.
2. The North Chukchi, Podvodnikov, Toll, Mendeleev, Nautilus, and Stefansson Basins formed synchronously with the AMR. In these basins, rifting-related, hyper-extension of continental crust accompanied by volcanism took place.
3. The region of the AMR and conjugate basins of Aptian-Albian age is a failed oceanic basin. The Amerasia Basin was an intraplate tectonic region in the Aptian-Albian.
4. The Alpha-Mendeleev Large Igneous Province originated during HALIP time (125–100 Ma with local prolongation up to 80 Ma) on pre-Cretaceous continental crust. SDR-like units dominate. The HAMH with high amplitude "chaotic" magnetic anomalies could be explained by regional distribution of SDRs and other magmatic and tectonic features.
5. At 100–56 Ma, the Mendeleev Rise was probably a submarine high with relatively slow, shallow-water sedimentation in bathymetric lows and a number of hiatuses on bathymetric highs. During 56–45 Ma, relative submarine highs were covered by shallow-water carbonates including buildups. At ~ 45 Ma, vertical movements started with formation of normal faults in a transtensional setting together with the onset of rapid subsidence. At ~ 20 Ma regional rapid subsidence started with increasing water depth ultimately exceeding 1500 m.
6. The North Chukchi Basin has a sedimentary cover thickness of up to ~ 20 km. Postrift sediments younger than 100 Ma cover its highly stretched continental acoustic basement in the central part. The Basin formed simultaneously with the Mendeleev Rise. Postrift deposits in the North Chukchi Basin cover the southern continuation of the Mendeleev Rise as the Kucherov High.
7. The North Amerasia (Alpha-Mendeleev) domain was affected by normal faulting after HALIP time during two phases at least. During the late Cretaceous (~80–66 Ma) a system of normal faults and grabens formed in a large region of the Stefansson and Canada basins including Sever Spur and the Alpha Ridge slope. Normal faulting took place in the AMR after 45 Ma.

Uncited references

Helwig et al. (2011), Jakobsson et al. (2012), Jokat (2005), Kumar et al. (2011), Nikishin et al. (2018), Rekant et al. (2015), Shipilov (2016), Skolotnev et al. (2017).

Declaration of Competing Interest

The authors declare that they have no known competing financial interests or personal relationships that could have appeared to influence the work reported in this paper.

Acknowledgements

The authors are grateful to the Ministry of Natural Resources and Environment of the Russian Federation, the Federal Subsoil Resources Management Agency, and Rosgeo for the opportunity to publish this paper. E. Lundin, G. Leitchenkov, L. Geoffroy, D. Franke, D. Zastrozhnov, P. Werner, L. Gernigon, E. Weigelt gave us important recommendations for improvement of seismic data interpretation. We thank S. Cloetingh and R. Stephenson, who studied our paper and gave a number of comments. Key ideas of the paper were discussed with D. Mosher, J. Shimeld, and C. Gaina. We thank the reviewers for generous, detailed, and constructive criticism and editing of out text. This study was supported by the Russian Science Foundation (Grant 22-27-00160).

Appendix A. Supplementary data

Supplementary data to this article can be found online at https://doi.org/10.1016/j.gr.2022.10.010.

References

Abdelmalak, M.M., Andersen, T.B., Planke, S., Faleide, J.I., Corfu, F., Tegner, C., Shephard, G.E., Zastrozhnov, D., Myklebust, R., 2015. The ocean-continent transition in the mid-Norwegian margin: Insight from seismic data and an onshore Caledonian field analogue. Geology 43 (11), 1011–1014. https://doi.org/10.1130/G37086.1.

Alvey, A., Gaina, C., Kusznir, N.J., Torsvik, T.H., 2008. Integrated crustal thickness mapping and plate reconstructions for the high Arctic. Earth Planet. Sci. Lett. 274, 310–321. https://doi.org/10.1016/j.epsl.2008.07.036.

Andronikov, A., Mukasa, S., Mayer, L.A. & Brumley, K., 2008. First Recovery of Submarine Basalts from the Chukchi Borderland and Alpha/Mendeleev Ridge region, Arctic Ocean. EOS Transactions, American Geophysical Union, 89, Fall Meeting Supplement, Abstract V41D-2124.

Backman, J., Jakobsson, M., Frank, M., Sangiorgi, F., Brinkhuis, H., Stickley, C., O'Regan, M., Løvlie, R., Pälike, H., Spofforth, D., Gattacecca, J., Moran, K., King, J., Heil, C., 2008. Age model and core-seismic integration for the Cenozoic Arctic Coring Expedition sediments from the Lomonosov Ridge. Paleoceanography 23, n/a-n/a. https://doi.org/10.1029/2007PA001476.

Backman, J., Moran, K., 2009. Expanding the Cenozoic paleoceanographic record in the Central Arctic Ocean: IODP Expedition 302 Synthesis. Open Geosci. 1. https://doi.org/10.2478/v10085-009-0015-6.

Biari, Y., Klingelhoefer, F., Franke, D., Funck, T., Loncke, L., Sibuet, J.-C., Basile, C., Austin, J.A., Rigoti, C.A., Sahabi, M., Benabdellouahed, M., Roest, W.R., 2021. Structure and evolution of the Atlantic passive margins: A review of existing rifting models from wide-angle seismic data and kinematic reconstruction. Mar. Petrol. Geol. 126, 104898. https://doi.org/10.1016/j.marpetgeo.2021.104898.

Brocher, T.M., 2005. Empirical Relations between Elastic Wavespeeds and Density in the Earth's Crust. Bull. Seismolog. Society Soc. of America. 95 (6), 2081–2092.

Brumley, K., 2014. Geologic history of the Chukchi Borderland. Stanford University, Arctic Ocean. http://purl.stanford.edu/hz857zk1405.

Brumley, K., Miller, E.L., Konstantinou, A., Grove, M., Meisling, K.E., Mayer, L.A., 2015. First bedrock samples dredged from submarine outcrops in the Chukchi Borderland, Arctic Ocean. Geosphere 11, 76–92. https://doi.org/10.1130/GES01044.1.

Bruvoll, V., Kristoffersen, Y., Coakley, B.J., Hopper, J.R., 2010. Hemipelagic deposits on the Mendeleev and northwestern Alpha submarine Ridges in the Arctic Ocean: acoustic stratigraphy, depositional environment and an inter-ridge correlation calibrated by the ACEX results. Mar. Geophys. Res. 31, 149–171. https://doi.org/10.1007/s11001-010-9094-9.

Bruvoll, V., Kristoffersen, Y., Coakley, B.J., Hopper, J.R., Planke, S., Kandilarov, A., 2012. The nature of the acoustic basement on Mendeleev and northwestern Alpha ridges, Arctic Ocean. Tectonophysics 514–517, 123–145. https://doi.org/10.1016/j.tecto.2011.10.015.

Buchan, K.L., Ernst, R.E., 2018. A giant circumferential dyke swarm associated with the High Arctic Large Igneous Province (HALIP). Gondwana Res. 58, 39–57. https://doi.org/10.1016/j.gr.2018.02.006.

Buck, W.R., 2017. The role of magmatic loads and rift jumps in generating seaward dipping reflectors on volcanic rifted margins. Earth Planet. Sci. Lett. 466, 62–69. https://doi.org/10.1016/j.epsl.2017.02.041.

Butsenko, V.V., Poselov, V.A., Zholondz, S.M., Smirnov, O.E., 2019. Seismic Attributes of the Podvodnikov Basin Basement. Doklady Earth Sci. 488, 1182–1185. https://doi.org/10.1134/S1028334X19100015.

Chauvet, F., Sapin, F., Geoffroy, L., Ringenbach, J.-C., 2021. Conjugate volcanic passive margins in the austral segment of the South Atlantic – Architecture and development. Earth-Sci. Rev. 212, 103461. https://doi.org/10.1016/j.earscirev.2020.103461.

Chernykh, A.A., Astafurova, E.G., Glebovsky, V.Yu., Korneva, M.S., Egorova, A,V., Red'ko, A.G. 2016. New Data on Tectonics of Mendeleev Ridge and Adjacent Geological Structures. Doklady Earth Sciences, 2016, Vol. 470, Part 1, 900–904. DOI: 10.1134/S1028334X16090117.

Chernykh, A., Glebovsky, V., Zykov, M., Korneva, M., 2018. New insights into tectonics and evolution of the Amerasia Basin. J. Geodyn. 119, 167–182. https://doi.org/10.1016/j.jog.2018.02.010.

Chian, D., and N. Lebedeva-Ivanova (2015), Atlas of Sonobuoy velocity analyses in Canada Basin, edited by G. S. O. Canada, Ottawa. DOI: 10.4095/295857.

Chian, D., Jackson, H.R., Hutchinson, D.R., Shimeld, J.W., Oakey, G.N., Lebedeva-Ivanova, N., Li, Q., Saltus, R.W., Mosher, D.C., 2016. Distribution of crustal types in Canada Basin, Arctic Ocean. Tectonophysics 691, 8–30. https://doi.org/10.1016/j.tecto.2016.01.038.

Coakley, B., Brumley, K., Lebedeva-Ivanova, N., Mosher, D., 2016. Exploring the geology of the central Arctic Ocean; understanding the basin features in place and time. J. Geol. Soc. London. 173, 967–987. https://doi.org/10.1144/jgs2016-082.

Corfu, F., Polteau, S., Planke, S., Faleide, J.I., Svensen, H., Zayoncheck, A., Stolbov, N., 2013. U–Pb geochronology of cretaceous magmatism on Svalbard and Franz Josef Land, Barents Sea large Igneous Province. Geol. Mag. 150, 1127–1135. https://doi.org/10.1017/S0016756813000162.

Craddock, W.H., Houseknecht, D.W., 2016. Cretaceous-Cenozoic burial and exhumation history of the Chukchi shelf, offshore Arctic Alaska. Am. Assoc. Pet. Geol. Bull. 100, 63–100. https://doi.org/10.1306/09291515010.

Dobretsov, N.L., Vernikovsky, V.A., Karyakin, Y.V., Korago, E.A., Simonov, V.A., 2013. Mesozoic-Cenozoic volcanism and geodynamic events in the Central and Eastern Arctic. Russ. Geol. Geophys. 54, 874–887. https://doi.org/10.1016/j.rgg.2013.07.008.

Dockman, D.M., Pearson, D.G., Heaman, L.M., Gibson, S.A., Sarkar, C., 2018. Timing and origin of magmatism in the Sverdrup Basin, Northern Canada—Implications for lithospheric evolution in the High Arctic Large Igneous Province (HALIP). Tectonophysics 742–743, 50–65. https://doi.org/10.1016/j.tecto.2018.05.010.

Døssing, A., Jackson, H.R., Matzka, J., Einarsson, I., Rasmussen, T.M., Olesen, A.V., Brozena, J.M., 2013. On the origin of the Amerasia Basin and the High Arctic Large Igneous Province—Results of new aeromagnetic data. Earth Planet. Sci. Lett. 363, 219–230. https://doi.org/10.1016/j.epsl.2012.12.013.

Døssing, A., Gaina, C., Brozena, J.M., 2017. Building and breaking a large igneous province: An example from the High Arctic. Geophys. Res. Lett. 44, 6011–6019. https://doi.org/10.1002/2016GL072420.

Døssing, A., Gaina, C., Jackson, H.R., Andersen, O.B., 2020. Cretaceous ocean formation in the High Arctic. Earth Planet. Sci. Lett. 551, 116552. https://doi.org/10.1016/j.epsl.2020.116552.

Dove, D., Coakley, B., Hopper, J., Kristoffersen, Y., Team, H.G., 2010. Bathymetry, controlled source seismic and gravity observations of the Mendeleev ridge; implications for ridge structure, origin, and regional tectonics. Geophys. J. Int. 183, 481–502. 10.1111/j.1365-246X.2010.04746.x.

Drachev, S.S., Malyshev, N.A., Nikishin, A.M., 2010. Tectonic history and petroleum geology of the Russian Arctic Shelves: an overview. Geol. Soc. London. Pet. Geol. Conf. Ser. 7, 591–619. https://doi.org/10.1144/0070591.

Drachev, S.S., Mazur, S., Campbell, S., Green, C., Tishchenko, A., 2018. Crustal architecture of the East Siberian Arctic Shelf and adjacent Arctic Ocean constrained by seismic data and gravity modeling results. J. Geodyn. 119, 123–148. https://doi.org/10.1016/j.jog.2018.03.005.

Evangelatos, J., Funck, T., Mosher, D.C., 2017. The sedimentary and crustal velocity structure of Makarov Basin and adjacent Alpha Ridge. Tectonophysics 696–697, 99–114. https://doi.org/10.1016/j.tecto.2016.12.026.

Evangelatos, J., Mosher, D.C., 2016. Seismic stratigraphy, structure and morphology of Makarov Basin and surrounding regions: tectonic implications. Mar. Geol. 374, 1–13. https://doi.org/10.1016/j.margeo.2016.01.013.

Firth, J.V., Clark, D.L., 1998. An early Maastrichtian organic-walled phytoplankton cyst assemblage from an organic-rich black mud in Core Fl-533, Alpha Ridge: evidence for upwelling conditions in the Cretaceous Arctic Ocean. Marine Mar. Micropaleontol. 34, 1–27.

Foulger, G.R., Doré, T., Emeleus, C.H., Franke, D., Geoffroy, L., Gernigon, L., Hey, R., Holdsworth, R.E., Hole, M., Höskuldsson, Á., Julian, B., Kusznir, N., Martinez, F., McCaffrey, K.J.W., Natland, J.H., Peace, A.L., Petersen, K., Schiffer, C., Stephenson, R., Stoker, M., 2020. The Iceland Microcontinent and a continental Greenland-Iceland-Faroe Ridge. Earth- Sci. Rev. 206. https://doi.org/10.1016/j.earscirev.2019.102926.

Foulger, G.R., Gernigon, L., and Geoffroy, L., 2022, Icelandia, in Foulger, G.R., Hamilton, L.C., Jurdy, D.M., Stein, C.A., Howard, K.A., and Stein, S., eds., In the Footsteps of Warren B. Hamilton: New Ideas in Earth Science: Geol. Soc. of America Spec. Paper 553, p 10.1130/2021.2553(04).

Franke, D., 2013. Rifting, lithosphere breakup and volcanism: Comparison of magma-poor and volcanic rifted margins. Mar. Petrol. Geol. 43, 63–87. https://doi.org/10.1016/j.marpetgeo.2012.11.003.

Franke, D., Hinz, K., 2005. The structural style of sedimentary basins on the shelves of the Laptev Sea and the western East Siberian Sea, Siberian Arctic. J. Petrol. Geol. 28 (3), 269–286.

Funck, T., Shimeld, J., Salisbury, M.H. 2022. Magmatic and rifting-related features of the Lomonosov Ridge, and relationships to the continent-ocean transition zone in the Amundsen Basin, Arctic Ocean. Geophys. J. Inter., 2022;, ggab501, 10.1093/gji/ggab501.

Funck, T., Jackson, H.R., Shimeld, J., 2011. The crustal structure of the Alpha Ridge at the transition to the Canadian Polar Margin: Results from a seismic refraction experiment. J. Geophys. Res. 116, B12101. https://doi.org/10.1029/2011JB008411.

Gaina, C., Werner, S.C., Saltus, R., Maus, S., 2011. Chapter 3 Circum-Arctic mapping project: new magnetic and gravity anomaly maps of the Arctic. Geol. Soc. London, Mem. 35, 39–48. 10.1144/M35.3.
Gaina, C., Medvedev, S., Torsvik, T.H., Koulakov, I., Werner, S.C., 2014. 4D Arctic: A Glimpse into the Structure and Evolution of the Arctic in the Light of New Geophysical Maps, Plate Tectonics and Tomographic Models. Surv. Geophys. 35, 1095–1122. https://doi.org/10.1007/s10712-013-9254-y.
Gakkel, Ya. Ya. 1962. The exploration and development of polar lands, in Harris, C.D., ed., Soviet geography: Accomplishments and tasks: New York, American Am. Geographical Geograph. Society Soc. Occasional Publication Publ. 1, p. 265–274.
Gardner, G.H.F., Gardner, L.W., Gregory, A.R., 1974. Formation velocity and density - the diagnostic basics for stratigraphic traps. Geophysics 39, 770–780.
Geoffroy, L., 2005. Volcanic passive margins. Comptes Rendus Geosci. 337, 1395–1408. https://doi.org/10.1016/j.crte.2005.10.006.
Geoffroy, L., Burov, E.B., Werner, P., 2015. Volcanic passive margins: another way to break up continents. Sci. Reports. 5, 14828. https://doi.org/10.1038/srep14828.
Geoffroy, L., Guan, H., Foulger, G.R., Werner, P. 2020. The Extent of Continental Material in Oceans: C-Blocks and the Laxmi Basin Example. Geoph. J. Inter., doi: 10.1093/gji/ggaa215.
Geoffroy, L., Gernigon, L. and Foulger, G.R., 2022. Linear magnetic anomalies and the limits of oceanic crust in oceans. In: G.R. Foulger, D.M. Jurdy, C.A. Stein, L.C. Hamilton, K. Howard and S. Stein (Editors), In the Footsteps of Warren B. Hamilton: New Ideas in Earth Science. Geological Society of America, Boulder, CO, Doi: 10.1130/2021.2553(04).
Glebovsky, V.Y., Astafurova, E.G., Chernykh, A.A., Korneva, M.A., Kaminsky, V.D., Poselov, V.A., 2013. Thickness of the Earth's crust in the deep Arctic Ocean: Results of a 3D gravity modeling. Russ. Geol. Geophys. 54, 247–262. https://doi.org/10.1016/j.rgg.2013.02.001.
Grantz, A., Clark, D.L., Phillips, R.L., Srivastava, S.P., Blome, C.D., Gray, L.B., Haga, H., Mamet, B.L., McIntyre, D.J., McNeil, D.H., Mickey, M.B., Mullen, M.W., Murchey, B.I., Ross, C.A., Stevens, C.H., Silberling, N.J., Wall, J.H., Willard, D.A., 1998. Phanerozoic stratigraphy of Northwind Ridge, magnetic anomalies in the Canada basin, and the geometry and timing of rifting in the Amerasia basin, Arctic Ocean. Geol. Soc. Amer. Bull. 110 (6), 801–820.
Grantz, A., Hart, P. & Childers, V. 2011. Geology and tectonic development of the Amerasia and Canada Basins, Arctic Ocean. In: Spencer, A.M., Embry, A. F., Gautier, D.L., Stoupakova, A.V. & Sørensen, K. (eds) Arctic Petroleum Geology. Geol. Soc., London, Mem., 35, 771–799, http://doi.org/ 10.1144/M35.50.
Grantz, A., Scott, R.A., Drachev, S.S., Moore, T.E., Valin, Z.C., 2011. Chapter 2 Sedimentary successions of the Arctic Region (58–64° to 90°N) that may be prospective for hydrocarbons. Geol. Soc. London, Mem. 35, 17–37. 10.1144/M35.2.
Guan, H., Geoffroy, L., Gernigon, L., Chauvet, F., Grigné, C., 2019. Magmatic ocean-continent transitions. Mar. Petrol. Geol. 104, 438–450. https://doi.org/10.1016/j.marpetgeo.2019.04.003.
Hadlari, T., Issler, D.R., 2019. Late Cretaceous uplift of northern Axel Heiberg Island, Nunavut, revealed by apatite fission track data, and a schematic model related to Baffin Bay extension. Geol. Survey Canada, Open File 8494, 98 p. https://doi.org/10.4095/313399.
Harkin, C., Kusznir, N., Roberts, A., Manatschal, G., Horn, D., 2020. Origin, composition and relative timing of seaward dipping reflectors on the Pelotas rifted margin. Marine Petrol. Geol. 114, 104235. https://doi.org/10.1016/j.marpetgeo.2020.104235.
Harrison, J.C., St-Onge, M.R., Petrov, O.V., Strelnikov, S.I., Lopatin, B.G., Wilson, F.H., Tella, S., Paul, D., Lynds, T., Shokalsky, S.P., Hults, C.K., Bergman, S., Jepsen, H.F., Solli, A., 2011. Geological map of the Arctic; Geological Survey of Canada, Map 2159A, scale 1:5 000 000. Geological Survey of Canada.
Heezen, B.C., Tharp, M. 1975. Map of the Arctic Region. World 1 : 5 000 000. American Geographical Society.
Hegewald, A., Jokat, W., 2013. Tectonic and sedimentary structures in the northern Chukchi region, Arctic Ocean. J. Geophys. Res. Solid Earth 118, 3285–3296. https://doi.org/10.1002/jgrb.50282.
Helwig, J., Kumar, N., Emmet, P., Dinkelman, M.G., 2011. Chapter 35 Regional seismic interpretation of crustal framework, Canadian Arctic passive margin, Beaufort Sea, with comments on petroleum potential. Geol. Soc. London, Mem. 35, 527–543. 10.1144/M35.35.
Homza, T.X., Bergman, S.C., 2019. A Geologic Interpretation of the Chukchi Sea Petroleum Province: Offshore Alaska, USA. Am. Ass. Petrol. Geologists. 10.1306/AAPG119.
Hunkins, K.L., 1961. Seismic studies of the Arctic Ocean floor. Geol. Arctic 1, 645–665.
Hutchinson, D.R., Jackson, H.R., Houseknecht, D.W., Li, Q., Shimeld, J.W., Mosher, D.C., Chian, D., Saltus, R.W., Oakey, G.N., 2017. Significance of Northeast-Trending Features in Canada Basin, Arctic Ocean. Geochem., Geophys. Geosyst. 18, 4156–4178. https://doi.org/10.1002/2017GC007099.
Ilhan, I., Coakley, B.J., 2018. Meso-Cenozoic evolution of the southwestern Chukchi Borderland, Arctic Ocean. Mar. Petrol. Geol. 95, 100–109. https://doi.org/10.1016/j.marpetgeo.2018.04.014.
Jackson, H.R., Chian, D. 2019. The Alpha-Mendeleev ridge a large igneous province with continental affinities. GFF, DOI: 10.1080/11035897.2019.1655789
Jackson, H.R., Forsyth, D.A., Johnson, G.L., 1986. Oceanic affinities of the Alpha Ridge, Arctic Ocean. Mar. Geol. 73, 237–261.
Jakobsson, M., Backman, J., Rudels, B., Nycander, J., Frank, M., Mayer, L., Jokat, W., Sangiorgi, F., O'Regan, M., Brinkhuis, H., King, J., Moran, K., 2007. The early Miocene onset of a ventilated circulation regime in the Arctic Ocean. Nature 447, 986–990. https://doi.org/10.1038/nature05924.
Jakobsson, M., Mayer, L., Coakley, B., Dowdeswell, J.A., Forbes, S., Fridman, B., Hodnesdal, H., Noormets, R., Pedersen, R., Rebesco, M., Schenke, H.W., Zarayskaya, Y., Accettella, D., Armstrong, A., Anderson, R.M., Bienhoff, P., Camerlenghi, A., Church, I., Edwards, M., Gardner, J.V., Hall, J.K., Hell, B., Hestvik, O., Kristoffersen, Y., Marcussen, C., Mohammad, R., Mosher, D., Nghiem, S.V., Pedrosa, M.T., Travaglini, P.G., Weatherall, P., 2012. The International Bathymetric Chart of the Arctic Ocean (IBCAO) Version 3.0. Geophys. Res. Lett. 39, n/a-n/a. https://doi.org/10.1029/2012GL052219.
Jakobsson, M., Mayer, L.A., Bringensparr, C., et al., 2020. The International Bathymetric Chart of the Arctic Ocean Version 4.0. Sci Data 7, 176. https://doi.org/10.1038/s41597-020-0520-9.
Jokat, W., 2003. Seismic investigations along the western sector of Alpha Ridge, Central Arctic Ocean. Geophys. J. Int. 152, 185–201. https://doi.org/10.1046/j.1365-246X.2003.01839.x.
Jokat, W., 2005. The sedimentary structure of the Lomonosov Ridge between 88°N and 80°N. Geophys. J. Int. 163, 698–726. https://doi.org/10.1111/j.1365-246X.2005.02786.x.
Jokat, W., Stein, R., Rachor, E. & Schewe, I. & the Shipboard Scientific Party 1999. Expedition gives fresh view of Central Arctic geology. EOS Transactions, American Geophysical Union, 80, 472–473.
Jokat, W., Ickrath, M., O'Connor, J., 2013. Seismic transect across the Lomonosov and Mendeleev Ridges: Constraints on the geological evolution of the Amerasia Basin, Arctic Ocean. Geophys. Res. Lett. 40, 5047–5051. https://doi.org/10.1002/grl.50975.
Jokat, W., Ickrath, M., 2015. Structure of ridges and basins off East Siberia along 81°N, Arctic Ocean. Mar. Petrol. Geol. 64, 222–232. https://doi.org/10.1016/j.marpetgeo.2015.02.047.
Jokat, W., Uenzelmann-Neben, G., Kristoffersen, Y., Rasmussen, T.M., 1992. Lomonosov Ridge-A double-sided continental margin. Geology 20, 887–890.
Kashubin, S.N., Petrov, O.V., Artemieva, I.M., Morozov, A.F., Vyatkina, D.V., Golysheva, Y.S., Kashubina, T.V., Milshtein, E.D., Rybalka, A.V., Erinchek, Y.M., Sakulina, T.S., Krupnova, N.A., Shulgin, A.A., 2018. Crustal structure of the Mendeleev Rise and the Chukchi Plateau (Arctic Ocean) along the Russian wide-angle and multichannel seismic reflection experiment "Arctic-2012". J. Geodyn. 119, 107–122. https://doi.org/10.1016/j.jog.2018.03.006.
Knudsen, C., Hopper, J.R., Bierman, P.R., Bjerager, M., Funck, T., Green, P.F., Ineson, J.R., Japsen, P., Marcussen, C., Sherlock, S.C., Thomsen, T.B., 2018. Samples from the Lomonosov Ridge place new constraints on the geological evolution of the Arctic Ocean. Geol. Soc. London Spec. Publ. 460, 397–418. https://doi.org/10.1144/SP460.17.
Kossovaya, O.L., Tolmacheva, T.Y., Petrov, O.V., Isakova, T.N., Ivanova, R.M., Mirolyubova, E.S., Rekant, P.V., Gusev, E.A., 2018. Palaeozoic carbonates and fossils of the Mendeleev Rise (Eastern Arctic): study of sea bottom dredged material. J. Geodyn. 120, 23–44. https://doi.org/10.1016/j.jog.2018.05.001.
Kumar, N., Granath, J.W., Emmet, P.A., Helwig, J.A., Dinkelman, M.G., 2011. Chapter 33 Stratigraphic and tectonic framework of the US Chukchi Shelf: exploration insights from a new regional deep-seismic reflection survey. Geol. Soc. London, Mem. 35, 501–508. 10.1144/M35.33.
Lang, G., ten Brink, U.S., Hutchinson, D.R., Mountain, G.S., Schattner, U., 2020. The role of pre-magmatic rifting in shaping a volcanic continental margin: An example from the Eastern North American Margin. J. Geophys. Res.: Solid Earth. https://doi.org/10.1002/essoar.10502270.2.
Langinen, A.E., Lebedeva-Ivanova, N.N., Gee, D.G., Zamansky, Y.Y., 2009. Correlations between the Lomonosov Ridge, Marvin Spur and adjacent basins of the Arctic Ocean based on seismic data. Tectonophysics 472, 309–322. https://doi.org/10.1016/j.tecto.2008.05.029.
Laverov, N.P., Lobkovsky, L.I., Kononov, M.V., Dobretsov, N.L., Vernikovsky, V.A., Sokolov, S.D., Shipilov, E.V., 2013. A geodynamic model of the evolution of the Arctic basin and adjacent territories in the Mesozoic and Cenozoic and the outer limit of the Russian Continental Shelf. Geotectonics 47, 1–30. https://doi.org/10.1134/S0016852113010044.
Lebedeva-Ivanova, N.N., Gee, D.G., Sergeyev, M.B., 2011. Chapter 26 Crustal structure of the East Siberian continental margin, Podvodnikov and Makarov basins, based on refraction seismic data (TransArctic 1989–1991). Geol. Soc. London, Mem. 35, 395–411. 10.1144/M35.26.
Lebedeva-Ivanova, N., Gaina, C., Minakov, A., Kashubin, S., 2019. ArcCRUST: Arctic Crustal Thickness From 3-D Gravity Inversion. Geochemistry, Geophys. Geosystems 2018GC008098. 10.1029/2018GC008098
Lebedeva-Ivanova, N.N., Zamansky, Y.Y., Langinen, A.E., Sorokin, M.Y., 2006. Seismic profiling across the Mendeleev Ridge at 82∘N: evidence of continental crust. Geophys. J. Int. 165, 527–544. https://doi.org/10.1111/j.1365-246X.2006.02859.x.
Li, L., Stephenson, R., Clift, P.D., 2016. The Canada Basin compared to the southwest South China Sea: Two marginal ocean basins with hyper-extended continent-ocean transitions. Tectonophysics 691, 171–184. https://doi.org/10.1016/j.tecto.2016.02.042.
Lobkovsky, L.I., Shipilov, E.V., Sorokhtin, N.O., 2021. Crustal Sinking and Formation of the Main Tectonic Structures and Igneous Provinces in the Arctic in the Late Cretaceous–Cenozoic: A View from the Subduction–Convective Model. Doklady Earth Sciences, Vol. 501, Part 1, pp. 901–905. DOI: 10.1134/S1028334X21110076
Matthews, K.J., Matthews, M., Müller, R.D., 2012. A global-scale plate reorganization event at 105–100 Ma. Earth Planet. Sci. Lett. 355–356, 283–298. https://doi.org/10.1016/j.epsl.2012.08.023.
McDermott, C., Lonergan, L., Collier, J.S., McDermott, K.G., Bellingham, P., 2018. Characterization of Seaward-Dipping Reflectors Along the South American Atlantic Margin and Implications for Continental Breakup. Tectonics 37, 3303–3327. https://doi.org/10.1029/2017TC004923.
McDermott, C., Collier, J.S., Lonergan, L., Fruehn, J., Bellingham, P., 2019. Seismic velocity structure of seaward-dipping reflectors on the South American continental margin. Earth Planet. Sci. Lett. 521, 14–24. https://doi.org/10.1016/

j.epsl.2019.05.049.

Miller, E.L., Akinin, V.V., Dumitru, T.A., Gottlieb, E.S., Grove, M., Meisling, K., Seward, G., 2018a. Deformational history and thermochronology of Wrangel Island, East Siberian Shelf and coastal Chukotka, Arctic Russia. Geol. Soc. London Spec. Publ. 460, 207–238. https://doi.org/10.1144/SP460.7.

Miller, E.L., Meisling, K.E., Akinin, V.V., Brumley, K., Coakley, B.J., Gottlieb, E.S., Hoiland, C.W., O'Brien, T.M., Soboleva, A., Toro, J., 2018b. Circum-Arctic Lithosphere Evolution (CALE) Transect C: displacement of the Arctic Alaska-Chukotka microplate towards the Pacific during opening of the Amerasia Basin of the Arctic. Geol. Soc. London Spec. Publ. 460, 57–120. https://doi.org/10.1144/SP460.9.

Miller, E.L., Verzhbitsky, V.E., 2009. Structural studies near Pevek, Russia: implications for formation of the East Siberian Shelf and Makarov Basin of the Arctic Ocean. Stephan Mueller Spec. Publ. Ser. 4, 223–241. https://doi.org/10.5194/smsps-4-223-2009.

Morozov, A.F., Petrov, O.V., S.P., S., Kashubin, S.N., Kremenetsky, A.A., Shkatov, M.Y., Kaminsky, V.D., Gusev, E.A., Grikurov, G.E., Rekant, P.V., Shevchenko, S.S., Sergeev, S.A., Shatov, V.V., 2013. New geological data substantiating continental nature of region of Central-Arctic rises. Reg. Geol. i Metallog. 55, 34–55 (in Russian).

Mosher, D. and Hutchinson, D.R., 2019. Chapter 10, Canada Basin. In: Springer International Publishing AG, A. Piskarev et al. (eds.), Geologic Structures of the Arctic Basin, 10.1007/978-3-319-77742-9_10.

Mosher, D.C., Shimeld, J., Hutchinson, D., Chian, D., Lebedova-Ivanova, N., Jackson, R., 2012. Canada Basin revealed, in: Society of Petroleum Engineers - Arctic Technology Conference 2012. pp. 805–815.

Mudie, P.J., Stoffyn-Egli, P., Van Wagoner, N.A., 1986. Geological constraints for tectonic models of the Alpha Ridge. J. Geodyn. 6, 215–1136.

Mukasa, S.B., Andronikov, A., Brumley, K., Mayer, L.A., Armstrong, A., 2020. Basalts from the Chukchi Borderland: 40Ar/39Ar Ages and Geochemistry of submarine intraplate lavas dredged from the western Arctic Ocean. Am. Geophys. Union. https://doi.org/10.1029/2019JB017604.

Mutter, J.C., 1985. Seaward dipping reflectors and the continent-ocean boundary at passive continental margins. Tectonophysics 114, 117–131.

Nikishin, A.M., Petrov, E.I., Cloetingh, S., Freiman, S.I., Malyshev, N.A., Morozov, A.F., Posamentier, H.W., Verzhbitsky, V.E., Zhukov, N.N., Startseva, 2021c. Arctic Ocean Mega Project: Paper 3 – Mesozoic to Cenozoic geological evolution. Earth-Sci. Rev. 217. 103034. 10.1016/j.earscirev.2019.103034.

Nikishin, A.M., Malyshev, N.A., Petrov, E.I., 2014. Geological Structure and History of the Arctic Ocean. EAGE Publications bv. 10.3997/9789462821880

Nikishin, A.M., Petrov, E.I., Malyshev, N.A., Ershova, V.P., 2017. Rift systems of the Russian Eastern Arctic shelf and Arctic deep water basins: link between geological history and geodynamics. Geodyn. Tectonophys. 8, 11–43. https://doi.org/10.5800/GT-2017-8-1-0231.

Nikishin, A.M., Gaina, C., Petrov, E.I., Malyshev, N.A., Freiman, S.I., 2018. Eurasia Basin and Gakkel Ridge, Arctic Ocean: Crustal asymmetry, ultra-slow spreading and continental rifting revealed by new seismic data. Tectonophysics 746, 64–82. https://doi.org/10.1016/j.tecto.2017.09.006.

Nikishin, A.M., Startseva, K.F., Verzhbitsky, V.E., Cloetingh, S., Malyshev, N.A., Petrov, E.I., Posamentier, H., Freiman, S.I., Lineva, M.D., Zhukov, N.N., 2019. Sedimentary Basins of the East Siberian Sea and the Chukchi Sea and the Adjacent Area of the Amerasia Basin: Seismic Stratigraphy and Stages of Geological History. Geotectonics 53, 635–657. https://doi.org/10.1134/S0016852119060104.

Nikishin, A.M., Petrov, E.I., Cloetingh, S., Freiman, S.I., Malyshev, N.A., Morozov, A.F., Posamentier, H.W., Verzhbitsky, V.E., Zhukov, N.N., Startseva, K.F., Rodina, E.A., 2021b. Arctic Ocean Mega Project: Paper 2 – Arctic stratigraphy and regional tectonic structure. Earth-Sci. Rev. 217, 103581. https://doi.org/10.1016/j.earscirev.2021.103581.

Nikishin, A.M., Petrov, E.I., Cloetingh, S., Korniychuk, A.V., Morozov, A.F., Petrov, O.V., Poselov, V.A., Beziazykov, A.V., Skolotnev, S.G., Malyshev, N.A., Verzhbitsky, V.E., Posamentier, H.W., Freiman, S.I., Rodina, E.A., Startseva, K.F., Zhukov, N.N., 2021a. Arctic Ocean Mega Project: Paper 1 - Data collection. Earth-Sci. Rev. 217, 103559. https://doi.org/10.1016/j.earscirev.2021.103559.

Norcliffe, J.R., Paton, D.A., Mortimer, E.J., McCaig, A.M., Nicholls, H., Rodriguez, K., Hodgson, N., Van Der Spuy, D., 2018. Laterally Confined Volcanic Successions (LCVS); recording rift-jumps during the formation of magma-rich margins. Earth Planet. Sci. Lett. 504, 53–63. https://doi.org/10.1016/j.epsl.2018.09.033.

Oakey, G.N., Saltus, R.W., 2016. Geophysical analysis of the Alpha-Mendeleev ridge complex: Characterization of the High Arctic Large Igneous Province. Tectonophysics 691, 65–84. https://doi.org/10.1016/j.tecto.2016.08.005.

Paton, D.A., Pindell, J., McDermott, K., Bellingham, P., Horn, B., 2017. Evolution of seaward-dipping reflectors at the onset of oceanic crust formation at volcanic passive margins: Insights from the South Atlantic. Geology. https://doi.org/10.1130/G38706.1.

Pease, V., Drachev, S., Stephenson, R., Zhang, X., 2014. Arctic lithosphere — A review. Tectonophysics 628, 1–25. https://doi.org/10.1016/j.tecto.2014.05.033.

Petrov, O.V., Smelror, M. (eds.). 2021. Tectonics of the Arctic. Springer Geology. 10.1007/978-3-030-46862-0.

Petrov, O., Morozov, A., Shokalsky, S., Kashubin, S., Artemieva, I.M., Sobolev, N., Petrov, E., Ernst, R.E., Sergeev, S., Smelror, M., 2016. Crustal structure and tectonic model of the Arctic region. Earth-Sci. Rev. 154, 29–71. https://doi.org/10.1016/j.earscirev.2015.11.013.

Petrov, O.V., Smelror, M. (Eds.), 2019, Tectonostratigraphic Atlas of the Arctic (eastern Russia and adjacent areas). St. Petersburg, VSEGEI Press, p. 152.

Piskarev, A., Poselov, V., Kaminsky, V. (Eds.), 2019, Geologic Structures of the Arctic Basin. Springer International Publishing, Cham. https://doi.org/10.1007/978-3-319-77742-9.

Planke, S., Symonds, P.A., Alvestad, E., Skogseid, J., 2020. Seismic volcanostratigraphy of large-volume basaltic extrusive complexes on rifted margins. J. Geophys. Res. 105, 19335–19351.

Polteau, S., Hendriks, B.W.H., Planke, S., Ganerød, M., Corfu, F., Faleide, J.I., Midtkandal, I., Svensen, H.S., Myklebust, R., 2016. The Early Cretaceous Barents Sea Sill Complex: Distribution, 40Ar/39Ar geochronology, and implications for carbon gas formation. Palaeogeogr. Palaeoclimatol. Palaeoecol. 441, 83–95. https://doi.org/10.1016/j.palaeo.2015.07.007.

Posamentier, H.W., Laurin, P., Warmath, A., Purnama, M., and Drajat, D., 2010, Seismic Stratigraphy and Geomorphology of Oligocene to Miocene Carbonate Buildups, Offshore Madura, Indonesia in Morgan, W.A., George, A.D., Harris, P.M., Kupecz, J.A., and Sarg, J.F., eds., Cenozoic Carbonate Systems of Australasia: Society of Economic Paleontologists and Mineralogists Special Publication 95, p. 104-121.

Poselov, V.A., Avetisov, G.P., Butsenko, V.V., Zholondz, S.M., Kaminsky, V.D., Pavlov, S.P., 2012. The Lomonosov Ridge as a natural extension of the Eurasian continental margin into the Arctic Basin. Russ. Geol. Geophys. 53, 1276–1290. https://doi.org/10.1016/j.rgg.2012.10.002.

Poselov, V.A., Butsenko, V.V., Zholondz, S.M., Zholondz, A.S., Kireev, A.A., 2017. Seismic Stratigraphy of Sedimentary Cover in the Podvodnikov Basin and North Chukchi Trough. Doklady Earth Sciences, Vol. 474. Part 2, 688–691. https://doi.org/10.1134/S1028334X17060137.

Poselov, V.A., Verba, V.V., Zholondz, S.M., Butsenko, V.V., 2019. The rises of the Amerasia basin, arctic ocean, and possible equivalents in the Atlantic ocean. Okeanologia 59, 810–825. https://doi.org/10.31857/S0030-1574595810-825. . (in Russian).

Rekant, P., Sobolev, N., Portnov, A., Belyatsky, B., Dipre, G., Pakhalko, A., Kaban'kov, V., Andreeva, I., 2019. Basement segmentation and tectonic structure of the Lomonosov Ridge, arctic Ocean: Insights from bedrock geochronology. J. Geodyn. 128, 38–54. 10.1016/j.jog.2019.05.001.

Rekant, P.V., Petrov, O.V., Kashubin, S.N., Rybalka, A.V., Shokalsky, S.P., Petrov, E.O., Vinokurov, I.Y., Gusev, E.A., 2015. Geological history of sedimentary cover of deep-water part of the Arctic Basin according to seismic data. Reg. Geol. i Metallog. 55, 34–55. . in Russian.

Saltus, R.W., Miller, E.L., Gaina, C., Brown, P.J., 2011. Chapter 4 Regional magnetic domains of the Circum-Arctic: a framework for geodynamic interpretation. Geol. Soc. London, Mem. 35, 49–60. 10.1144/M35.4.

Savin, V.A., 2020. Earth crust structure of sedimentary basins of the Laptev and East Siberian seas based on geophysical modelling. VNIIOkeangeologia. http://dissovet.sbras.ru/SBdisdocs/savin2019/Диссертация_Савин%20В.А.pdf.

Shephard, G.E., Müller, R.D., Seton, M., 2013. The tectonic evolution of the Arctic since Pangea breakup: Integrating constraints from surface geology and geophysics with mantle structure. Earth-Sci. Rev. 124, 148–183. https://doi.org/10.1016/j.earscirev.2013.05.012.

Sherwood, K.W., Johnson, P.P., Craig, J.D., Zerwick, S.A., Lothamer, R.T., Thurston, D.K., Hurlbert, S.B., 2002. Structure and stratigraphy of the Hanna Trough, U.S. Chukchi Shelf, Alaska, in: Miller, E.L., Grantz, A., Klemperer, S.L. (Eds.), Special Paper 360: Tectonic Evolution of the Bering Shelf-Chukchi Sea-Artic Margin and Adjacent Landmasses. Geological Society of America, Boulder. Colorado, pp. 39–66. 10.1130/0-8137-2360-4.39.

Shimeld, J.W., Chian, D., Jackson, H.R., Hutchinson, D., Mosher, D.C., Wade, J.A., Chapman, C.B., 2011. Evidence for an important tectonostratigraphic seismic marker across Canada Basin and southern Alpha Ridge of the Arctic Ocean; Geological Survey of Canada. Open File 6822. https://doi.org/10.4095/289234.

Shimeld, J., Funck, T., Li, Q., Oakey, G.N., Boggild, K., Jackson, R. 2019. Tectono-magmatic elements of the Alpha Ridge and possible associations with the High Arctic Large Igneous Province. Chapman Conference on Large-scale Volcanism in the Arctic: The Role of the Mantle and Tectonics. Abstracts. https://agu.confex.com/agu/19chapman3/meetingapp.cgi/Paper/485055.

Shimeld, J., Boggild, K., Mosher, D.C., and Jackson, H.R., 2021. Reprocessed multi-channel seismic-reflection data set from the Arctic Ocean, collected using icebreakers between 2007-2011 and 2014-2016 for the Canadian Extended Continental Shelf program; Geological Survey of Canada, Open File 8850, 1 .zip file. 10.4095/329248.

Shipilov, E.V., 2016. Basaltic magmatism and strike-slip tectonics in the Arctic margin of Eurasia: evidence for the early stage of geodynamic evolution of the Amerasia Basin. Russ. Geol. Geophys. 57, 1668–1687. https://doi.org/10.1016/j.rgg.2016.04.007.

Skaryatin, M.V., Stavitskaya, V.N., Mazaeva, I.V., Zaytseva, S.A., Batalova, A.A., Moiseeva, R.Kh., Vinnikovskaya, E.V., Bulgakova, E.A., Malyshev, N.A., Verzhbitskiy, V.E., Obmetko, V.V., Borodulin A.A., 2021. Application of spatial offlap break trajectory analysis of the North Chukchi Trough clinoforms for hydrocarbon evaluation. OIJ-2021-02-040-045-RU. DOI: 10.24887/0028-2448-2021-2-40-45.

Skolotnev, S., Aleksandrova, G., Isakova, T., Tolmacheva, T., Kurilenko, A., Raevskaya, E., Rozhnov, S., Petrov, E., Korniychuk, A., 2019. Fossils from seabed bedrocks: Implications for the nature of the acoustic basement of the Mendeleev Rise (Arctic Ocean). Mar. Geol. 407, 148–163. https://doi.org/10.1016/j.margeo.2018.11.002.

Skolotnev, S.G., Fedonkin, M.A., Korniychuk, A.V., 2017. New data on the geological structure of the southwestern Mendeleev Rise, Arctic Ocean. Doklady Earth Sci. 476, 1001–1006. https://doi.org/10.1134/S1028334X17090173.

Skolotnev, S.G., Freiman, S.I., Khisamutdinova, A.I., Ermolaev, B.V., Okina, O.I., Skolotneva, T.S., 2022. Sedimentary Rocks in the Basement of the Alpha-Mendeleev Rise, Arctic Ocean. Lithol. Mineral Resour. 57 (2), 121–142. https://doi.org/10.1134/S0024490222020079.

Stein, R., 2019. The late Mesozoic-Cenozoic Arctic Ocean climate and sea ice history: A challenge for past and future scientific ocean drilling. Paleoceanogr. Paleoclimatol. 34, 1851–1894. https://doi.org/10.1029/2018PA003433.

Stica, J.M., Zalán, P.V., Ferrari, A.L., 2014. The evolution of rifting on the volcanic margin of the Pelotas Basin and the contextualization of the Paranáe-Etendeka LIP in the separation of Gondwana in the South Atlantic. Marine Petrol. Geol. 50, 1–21. https://

doi.org/10.1016/j.marpetgeo.2013.10.015.
Struijk, E.L.M., Tesauro, M., Lebedeva-Ivanova, N., Gaina, C., Beekman, F., Cloetingh, S., 2018. The Arctic lithosphere: Thermo-mechanical structure and effective elastic thickness. Global Planet. Change 171, 2–17. https://doi.org/10.1016/j.gloplacha.2018.07.014.
Van Wagoner, N.A., Williamson, M.-C., Robinson, P.T., Gibson, I.L., 1986. First samples of acoustic basement recovered from the Alpha Ridge, Arctic Ocean: new constraints for the origin of the ridge. J. Geodyn. 6, 177–196.
Vernikovsky, V.A., Morozov, A.F., Petrov, O. V., Travin, A. V., Kashubin, S.N., Shokal'sky, S.P., Shevchenko, S.S., Petrov, E.O., 2014. New data on the age of dolerites and basalts of Mendeleev Rise (Arctic Ocean). Doklady Earth Sci. 454, 97–101. 10.1134/S1028334X1402007X.
Weber, J.R., 1986. The Alpha Ridge: gravity, seismic and magnetic evidence for a homogenous, mafic crust. J. Geodyn. 6, 117–136.
Weigelt, E., Jokat, W., Franke, D., 2014. Seismostratigraphy of the Siberian Sector of the Arctic Ocean and adjacent Laptev Sea Shelf. J. Geophys. Res. Solid Earth 119, 5275–5289. https://doi.org/10.1002/2013JB010727.
Weigelt, E., Jokat, W., Eisermann, H., 2020. Deposition history and paleo-current activity on the southeastern Lomonosov Ridge and its Eurasian flank based on seismic data. Geochem., Geophys., Geosys. 21.
Williamson, M.-C., Kellett, D., Miggins, D., Koppers, A., Carey, R., Oakey, G., Weis, D., Jokat, W., Massey, E. 2019. Age and Eruptive Style of Volcanic Rocks Dredged from the Alpha Ridge, Arctic Ocean. Geophysical Research Abstracts. Vol. 21, EGU2019-6336, 2019. EGU General Assembly 2019.
Yuan, X., Korenaga, J., Holbrook, W.S., Kelemen, P.B., 2020. Crustal structure of the Greenland-Iceland Ridge from joint refraction and reflection seismic tomography. J. Geophys. Res.: Solid Earth 125. https://doi.org/10.1029/2020JB019847.
Ziegler, P.A., Cloetingh, S., 2004. Dynamic processes controlling evolution of rifted basins. Earth-Sci. Rev. 64, 1–50. https://doi.org/10.1016/S0012-8252(03)00041-2.